ALEXANDRU IOAN CUZA UNIVERSITY OF IASI

JOURNAL OF EXPERIMENTAL AND MOLECULAR BIOLOGY

Volume 26 Number 3 (2025)

ISSN 2601 – 6974

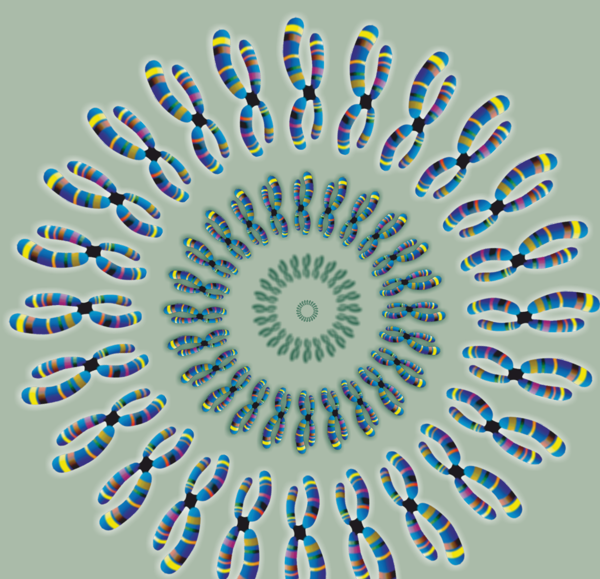

Alexandru Ioan Cuza University Publishing House

„ALEXANDRU IOAN CUZA" UNIVERSITY OF IAȘI

JOURNAL OF EXPERIMENTAL AND MOLECULAR BIOLOGY

TOME XXVI, Number 3 **2025**

Editura Universității „ALEXANDRU IOAN CUZA" din Iași

CONTENT

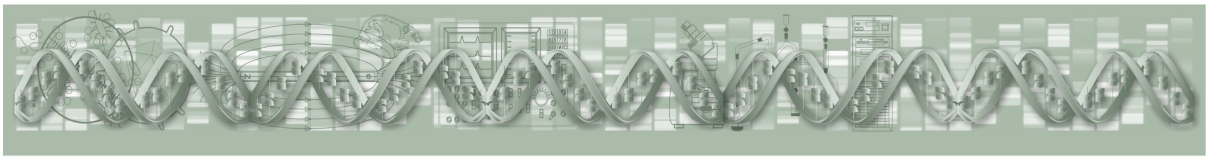

BIOCHEMICAL AND MOLECULAR CHARACTERIZATION OF STARTER CULTURES IN THE CONTROLLED FERMENTATION OF CABBAGE AND SOYBEANS

O.O. Tanko[1*], G.M. Gberikon[1], I.O. Ogbonna[1], T. Ichor[1], J.O. Olasan[1*]

[1]Department of Microbiology, Joseph Sarwuan Tarka University Makurdi, Nigeria
[*] Corresponding author e-mail: tankoodeni@gmail.com; olasan.olalekan@uam.edu.ng

Abstract

The aim of this study was to characterize starter cultures of LAB (lactic acid bacterium) and *Bacillus* spp. for controlled fermentation of cabbage and soybeans to achieve desired products. Cultured isolates were studied morphologically and revalidated using biochemical and molecular methods. Extracted DNA was amplified using two specific primers. Banding pattern at 1500bp showed the presence of LAB and *Bacillus subtilis* DNA amplified. La57 primer amplified amino acid antiporter gene that identified LAB while ENIF primer amplified endoglucanase gene that identified *B. subtilis.* The16S ribosomal RNA was sequenced using the Sanger's method for strain specific identification. As a result, the test organisms were morphologically identified as *Pediococcus* spp and *B. subtilis.* They differed in the type enzyme production (4:7 respectively). Sequence alignment identified them as *Pediococcus pentosaceus* strain DSM20336 (LAB) and *B. subtilis* subsp. *subtilis* strain 168. This is the novelty in this work. Results showed that *P. pentosaceus* induced ferments contained the least number of isolates in cabbage (*Lactobacillus* spp., *Streptococcus* spp. and *Pediococcus* spp) and soybean (*Bacillus* spp., *Streptococcus* spp. and *Pediococcus* spp) unlike in spontaneous fermentation where 8-9 bacterial isolates were recorded. The study identified potential fermenting strains of bacteria that could be employed as potential starter culture in the industrial fermentation of vegetable and legume foods to boost food security in Nigeria. These findings have industrial and economic benefits.
Keywords: Characterization, Starter Culture, Fermentation, Vegetable, Legume, Food security

Introduction

Industrial fermentation of foods has played major roles in boosting global food security. This is achieved through preservation and conversion of plant materials into diverse edible products that are available for people to choose from. Also, controlled fermentation increases the nutritional values of products (Walters et al. 2016).
In addition to traditional methods, modern techniques such as molecular characterization are now trending in the analysis of fermenters. They are concerned with specific identification of microbial strains and the genes responsible for fermentation of a particular food (Vossen et al. 2019). Techniques in extraction of genomic and plasmid DNA, PCR (Polymerase Chain Reaction), gradient gel electrophoresis, and 16s rDNA sequencing are employed to characterize different type food fermenters (Walters et al. 2016, Hui et al. 2017, Vossen et al. 2019). Characterization of isolates by using DNA fingerprinting electrophoresis has revealed genetic variability within highly heterogeneous species (Swain et al. 2014). Genetic variability has been

Received 6 December 2024; Reviewed 10 June 2025; Accepted 21 July 2025;
Published Online 21 July 2025; Published 30 September 2025

reported within a species of fermenting bacteria (Li et al. 2021). Knowledge of gene technology and genomics has played a major role in identification of new strains with potential fermenting capability of products and their use as probiotics (Li et al. 2021).

Identification of strains and variants of fermenting species of bacteria is very crucial in fermentation technology because of the need to ensure proper selection of starter culture needed to achieve desired results. Morphological identification of fermenters, that combines cultural and biochemical characterization, has been explored in this regard among authors (Emkani et al. 2022). This type of microbial systematic evidence provides baseline data of microbial identification that is limited to generic level and species taxa. However, starter culture needed in an elaborate fermentation of commercial product requires high level of microbial specificity and accuracy beyond species taxon. LAB and *Bacillus* spp. have been employed in the fermentation of vegetable and legume foods. However, lack of identity of strain specific variants make controlled fermentation experiments difficult to achieve. The aim of this study was to characterize starter cultures of a LAB and *Bacillus* spp. (in the controlled fermentation of cabbage and soybeans) using biochemical and molecular methods.

It was designed to explore the enzyme production differences and gene sequencing of 16s rDNA to identify the starter cultures to strain taxon.

Materials and Methods

Sample collection and preparation

Cabbage leaves and soybean seeds were purchased in sufficient quantities from major markets within the State Capital. All materials were packaged using sterile bags and transported to the laboratory for further processing and analysis. Cabbage leaves were cleaned by removing the damaged outer leaf cover. These were shredded after washing with sterile distilled water. Hydrated soybean seeds were dehulled manually by rubbing the seeds multiple times with the palms to get them ready for fermentation (Ahmad et al. 2015).

Source of organisms

LAB and *Bacillus* spp. were isolated from vegetable and legume sources. Stock cultures were also collected from the Microbiology Laboratory, Joseph Sarwuan Tarka University Makurdi, Nigeria. Sub-culturing was done on MRS agar using spread plate method followed by cultural characterization (Du et al. 2018).

Biochemical characterization of isolates

Isolates were revalidated using standard biochemical tests including Gram staining and enzyme production. The following tests were carried out: catalase, citrate utilization, urease, indole, amylase and gelatinase production tests using standard protocol as given by Florindo et al. (2018). Other enzyme production tests carried out were invertase, cellulase, lipase, phytase, protease and esterase tests. The bacteria isolates confirmed by biochemical tests were sub-cultured on Luria-Bertani (LB) media and incubated at 37°C overnight from which broth cultures were prepared for further revalidation and characterization using molecular techniques (Pino et al. 2018).

Extraction of genomic DNA

Protocols described in Du et al. (2018) and Arteaga et al. (2021) were used. Bacterial DNA was extracted using boiling method. Exactly 1.5ml of the sample broth was centrifuged at 10,000rpm for 5 min. The supernatant was decanted while the pellets were washed twice with 200µL sterile deionized water. This was followed by homogenization step and boiling in a water bath at 100°C for 10 min, while further centrifugation took place at 12,000 rpm for 5 min. The supernatant containing the DNA was transferred to another test tube and stored at -20°C. Purity of the extracted DNA was checked on a spectrophotometer at 280nm wavelength, using quantitative approach that determines the quantity of DNA extracted. This served as the template for PCR (Du et al. 2018, Arteaga et al. 2021).

Polymerase chain reaction (PCR)

This step amplified the extracted DNA (genomic and plasmid) of test isolates for a more precise identification than biochemical tests. The protocols outlined in Du et al. (2018) were used. Amplification was carried out on a thermocycler loaded with 50 µl reaction volumes containing; 25 ul Dream Taq Master Mix (Thermo Fisher Scientific, USA), 15µl of nuclease free water, 2.5µl of each primer and 2.5 µl of extracted bacterial DNA. The primers used in the amplification and their sequences are given in Table 1. The Amplification was done in 35 cycles with an initial denaturation at 95 ℃ for 5 min. followed by a denaturation step of 95 ℃ for 2 min, primer annealing at 55ºC for 30s and primer extension at 72℃ for 1 min, with the final extension at 72 ℃ for 10 min. The amplified DNA products were loaded on electrophoresis machine (64 V for 2 h) in a 1.5% agarose gel medium stained with ethidium bromide. Lamda DNA Hind III Marker was used as DNA molecular weight marker. Separated DNA bands were visualized on a UV trans-illuminator.

Gene sequencing and strains identification

All PCR products were purified with Exo sap for Sanger Dideoxy sequencing for determination of nucleotide arrangements in the genes and specific identification of strains of fermenting species of *Bacillus* and LAB. Variable regions within the 16s rRNA (ribosomal RNA) regions were sequenced. This was compared with known 16s rRNA sequence at National Centre for Biotechnology Information (NCBI) database using Basic Local Alignment Search Tool (BLASTn) algorithm using the online blast search at http://blast.ncbi.nlm.nih.gov/Blast.cgi. Identification of the sequences at both genus, species and strain level were defined as a 16s rRNA sequence similarity at between 95- 100% with that of the phenotype strain sequence in GenBank. (Du et al., 2018).

Table 1. List of Specific Primers for PCR

Primer	Gene function	Sequence	Base pair	Target
La57	Amino acid antiporter gene	F- GGTCGGGGGATCTGAAAAGA R- GATTTGGGCAAGCACATTGG	274	LAB (lactic acid bacteria)
EN1F	Endoglucanase gene	F-CCAGTAGCCAATGGCCAGC R-GGAATAATCGCCGCTTTGTGC	124	*Bacillus subtilis*

(Du et al. 2018, Arteaga et al. 2021)

Identification of bacterial species in fermented products

Controlled fermentation of cabbage and soybean experiments were set up using the characterized isolates as starter cultures. Spontaneous fermentation and bacterial induced fermentation were allowed to progress simultaneously. Morphological observations were recorded on the agar culture media. These included the colour and outline of the colony of each bacterium. Motility test was done by adding a drop of peptone water on a glass slide containing bacterial colony covered with a slip and viewed under the microscope with high power objective lens (Cheesbrough 2006). Serial dilution, pour plates techniques and incubation (37ºC for 24 hours) methods employed (Cheesbrough 2006). Visible colonies on the plates were counted using Colony Counter. Biochemical methods were used in analysis of bacterial species present in fermented products at week 4 of the experiment (Li et al. 2019) as previously discussed.

Results and discussions

Table 2 gives the morphological identification of isolates based on cultural and microscopic characterizations as well as responses to Gram's staining. Grey, circular Gram-positive rods that possessed smooth entire edge were typical of *B. subtilis.* Opaque, and circular Gram-positive rods with smooth entire edges were characteristics of *Pediococcus* species. Cultural characteristics of the isolates were in tandem with previous findings on morphologies of the test and standard cultures (Li et al. 2019). However, systematic resolutions were delimited to the genus taxon in *Pediococcus* and species taxon in *B. subtilis*. The study aligns with the use of cultural characteristics as fundamental steps, not only in providing pure culture for further analysis, but also in the determination of identity of the collected bacterial samples (Kiczorowski et al. 2022). Cultural characterization provides baseline information in microbial analysis of samples. All the LAB and *B. subtilis* were first identified using their outline, colour, transparency and elevation.

Table 2. Cultural and Microscopic Morphology of Bacterial Sample

Organism	Morphology	Gram reaction	Outline	Status
B. subtilis	Grey, Circular, Smooth, entire edge	+	Rods	Test colony
Pediococcus species	White/opaque circular and entire, tops of colonies were raised, convex or umbonate.	+	Rods	Test colony

Further biochemical characteristics re-validated the colonies according to their reactions to catalase, urease, citrate and indole tests (Table 3). *B. subtilis* colonies were positive to catalase and indole tests. Out of ten (10) enzymes screened for the test isolates (Table 4), *Pediococcus* spp produced 4 enzymes (amylase, lipase, phytase and protease) while *B. subtilis* produced 7 enzymes (catalase, urease, amylase, cellulase, lipase, phytase and gelatinase). The validity of the bacterial cultures confirmed through the use of basic biochemical tests gave credence to the identity of the LAB and *B. subtilis* tested. This aligns with standard bacteriological practices because it takes advantage of the biochemical and physiological responses of the isolates to certain chemical compounds. Unlike the cultural method of identification, biochemical methods are more objective and reliable (Adedokun et al. 2016, Pino et al. 2018, Taddia et al. 2019). Among other biochemical tests, enzyme production is a good biochemical parameter that distinguishes the test isolates.

Enzymes are organic catalysts that speed the rate of metabolic reactions in all living cells including microbial cells. The presence of functional enzymes is crucial in the formation of fermented food products. Production of these enzymes is an indicator of fermentative ability of the test isolates. This is because fermenters require functional enzymes to carry out food fermentation processes through hydrolysis, liquefaction, saccharification, and modification of diverse food types (Taddia et al. 2019). The above explanation probably accounts for the fermentation of cabbage and soybeans by LAB and *B. subtilis* used as starter culture in this work. According to Akanni et al. (2018), LAB produce lactic acid, organic acids and carbon dioxide during enzyme-based fermentation while *B. subtilis* hydrolyze proteins to form constituent peptides, amino acids and ammonia in alkaline fermentation. Fermentation enhances food digestibility and the level of vitamin, amino acids and minerals (Taddia et al. 2019).

Table 3. Biochemical Characteristics of Test and Standard Isolates

S/N	Biochemical tests	*B. subtilis*	*Pediococcus* species
1.	Catalase	+	-
2.	Urease	-	-
3.	Citrate	-	-
4.	Indole	+	-

Key: + = Positive, - = Negative

Table 4. Screening for Enzyme Production in Test Isolates

	Enzyme	*Pediococcus* spp.	*B. subtilis*
1	Catalase	Negative	Positive
2	Urease	Negative	Positive
3	Invertase	Negative	Negative
4	Amylase	Positive	Positive
5	Cellulase	Negative	Positive
6	Lipase	Positive	Positive
7	Phytase	Positive	Positive
8	Protease	Positive	Negative
9	Esterase	Negative	Negative
10	Gelatinase	Negative	Positive
Total		4 enzymes	7 enzymes

The two test isolates were confirmed true as shown in the agarose gel image that revealed DNA bands of the two bacteria (Plate 1). Banding pattern at 1500bp showed the presence of LAB and *B. subtilis* DNA amplified using two different specific primers. La57 primer amplified amino acid antiporter gene that identified LAB while ENIF primer amplified endoglucanase gene that identified *B. subtilis.* The sequence alignment of 16S ribosomal RNA of the test strain identified the LAB as *Pediococcus pentosaceus* strain DSM20336. It was assigned sequence identification number of 343201332|NR_042058.1. It contained 910 bits (1008) with 94% identity and 0% gaps. Sequence alignment of 16S ribosomal RNA of the test strain identified the *B. subtilis* as *B. subtilis* subsp. *subtilis* strain 168. It was assigned sequence identification number of 1269801457|NR-102783.2. It contained 426 bits (472) with 99% identity and 0% gaps.

Molecular characterization provides a more reliable confirmation and re-validation of test isolates at the gene level. This also confirms the presence of two genes (La57 coding for amino acid antiporter gene and EN1F gene coding for endoglucanase enzyme) needed in lactic acid and alkaline fermentation carried out by LAB and *B. subtilis* respectively. Starter culture needed in an elaborate fermentation of commercial product requires high level of microbial specificity and accuracy beyond species taxon (Walters et al. 2016, Hui et al. 2017). Identification of strains and variants of fermenting species of bacteria is very crucial in fermentation technology because of the need to ensure proper selection of starter culture needed to achieve desired results. In this work, sequence alignment of 16S ribosomal RNA of the test strain confirmed the LAB as *Pediococcus pentosaceus* strain DSM20336 and *B. subtilis* subsp. *subtilis* strain 168. These strains may offer potential use as probiotics in line with the recommendations of Vossen et al. (2019).

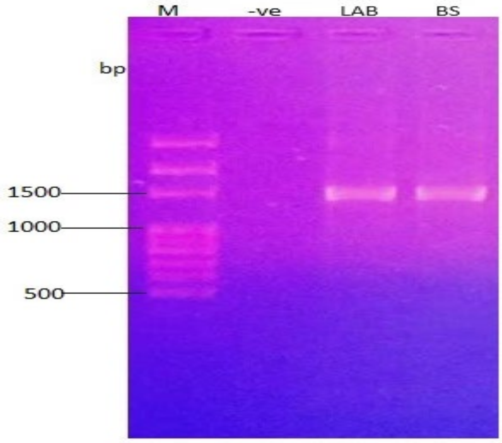

Plate 1. Agarose Gel Image of DNA Bands of LAB and *B. subtilis* Amplified by La57 and ENIF primers respectively
Legend: LAB (lactic acid bacteria); BS - *B. subtilis*

Figure 1 shows the number of bacterial isolates in fermented cabbage from week 1 to 4 of the experiments. Isolates consisted of 5-8 species in the first three weeks. In the final product (week 4), spontaneous fermented cabbage contained a total of 8 bacterial species of the genus *Bacillus, Escherichia*, *Staphylococcus*, *Pseudomonas*, *Micrococcus*, *Corynebacterium*, *Lactobacillus* and *Salmonella* (Table 5). Fermented cabbage with mixed culture of *Bacillus* + *Pediococcus* starter cultures contained 5 species: *Corynebacterium* spp., *Bacillus* spp., *Pediococcus* spp., *Leuconostoc* spp. and *Streptococcus* spp. Fermented cabbage with *B. subtilis* as starter culture contained 4 species of bacteria including *Bacillus* spp., *Streptococcus* spp., *Pediococcus* spp. and *Leuconostoc* spp. The 3 bacteria isolated from Pediococcus-ferment were *Lactobacillus* spp., *Streptococcus* spp. and *Pediococcus* spp.
There were evidences that unwanted bacteria were eliminated in cabbage and soybean ferments inoculated with single and mixed test strains especially when *P. pentosaceus* was applied as starter culture, thus confirming the antibacterial effects of the ferments. Results showed a clear elimination of *Escherichia*, *Staphylococcus*, *Pseudomonas*, *Micrococcus*, *Corynebacterium* and *Salmonella* found in products of spontaneous fermentation. These organisms were known to cause food spoilage and gastroenteric diseases. The present study conforms with the outcome of other studies since reports have shown that fermented vegetables and legumes may contain diverse micro-organisms strains of fermenting bacteria (Akanni et al. 2018, Kiczorowski et al. 2022).

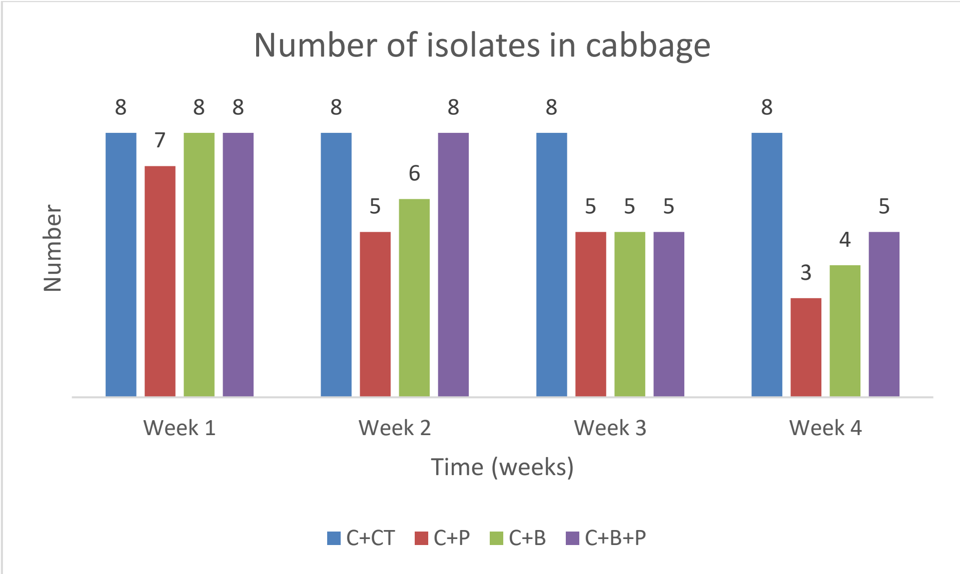

Figure 1. Number of Bacterial Isolates in Fermented Cabbage

Legend: C+CT= Control experiment (spontaneous fermentation); C+P = Cabbage + *Pediococcus*; C+B = Cabbage + *Bacillus*; C+B+P = Cabbage + *Bacillus* + *Pediococcus*

Table 5. Isolated Bacterial Species in Fermented Cabbage at Week 4

Treatments	C+CT	C+P	C+B	C+B+P
1	*Bacillus* spp.	*Lactobacillus* spp	*Bacillus* spp	*Corynebacterium* spp
2	*Escherichia coli*	*Streptococcus* spp	*Streptococcus* spp	*Bacillus* spp
3	*Staphylococcus* spp	*Pediococcus* spp	*Pediococcus* spp	*Pediococcus* spp
4	*Pseudomonas* spp		*Leuconostoc* spp	*Leuconostoc* spp
5	*Micrococcus* spp			*Streptococcus* spp
6	*Corynebacterium* spp			
7	*Lactobacillus* spp			
8	*Salmonella* spp			
Total isolates at week 4	8	3	4	5

Legend: C+CT= Control experiment (spontaneous fermentation); C+P = Cabbage + *Pediococcus*; C+B = Cabbage + *Bacillus* C+B+P = Cabbage + *Bacillus* + *Pediococcus*

Figure 2 shows the number of bacterial isolates in fermented soybeans from week 1 to 4 of the experiments. Isolates consisted of 4-9 species in the first three weeks. In the final product (week 4), spontaneously fermented soybean contained a total of 9 bacterial species of the genus *Bacillus, Escherichia*, *Staphylococcus*, *Pseudomonas*, *Micrococcus*, *Corynebacterium*, *Lactobacillus*, *Salmonella* and *Streptococcus* (Table 6). There were 5 species in two starter culture treated ferments: Bacillus+Pediococcus (S+B+P) ferment and Bacillus-ferment (S+B).

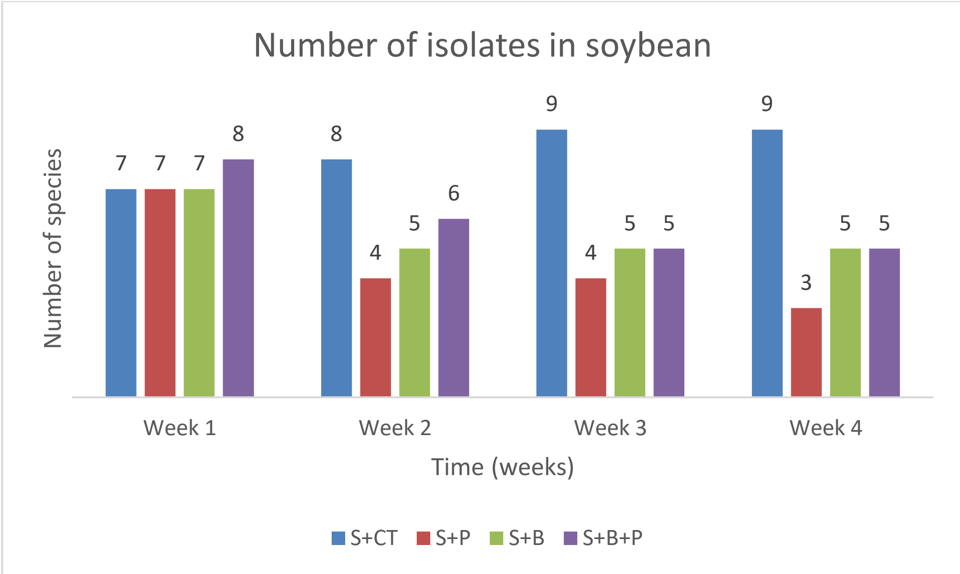

Figure 2. Number of Bacterial Isolates in Fermented Soybean
Legend: S+CT= Control experiment (spontaneous fermentation); S+P = Soybean + *Pediococcus*; S+B = Soybean + *Bacillus*; S+B+P = Soybean + *Bacillus* + *Pediococcus*

Table 6. Isolated Bacterial Species in Fermented Soybean at Week 4

Treatments	S+CT	S+P	S+B	S+B+P
1	*Bacillus* spp	*Bacillus* spp	*Bacillus* spp	*Lactobacillus* spp
2	*Escherichia coli*	*Streptococcus* spp	*Streptococcus* spp	*Bacillus* spp
3	*Staphylococcus* spp	*Pediococcus* spp	*Micrococcus* spp	*Pediococcus* spp
4	*Pseudomonas* spp		*Leuconostoc* spp	*Leuconostoc* spp
5	*Micrococcus* spp		*Lactobacillus* spp	*Streptococcus* spp
6	*Corynebacterium* spp			
7	*Lactobacillus* spp			
8	*Salmonella* spp			
9	*Streptococcus* spp			
Total at week 4	9	3	5	5

Legend: S+CT= Control experiment (spontaneous fermentation); S+P = Soybean + *Pediococcus*; S+B = Soybean + *Bacillus*; S+B+P = Soybean + *Bacillus* + *Pediococcus*

Although the aim of the study was achieved, some limitations were noted. These were lack of strain identity of the bacterial isolates as unwanted contaminants present as the experiment progressed, inability to introduce quality control points to eliminate undesired bacteria and lack of controlled optimized conditions for fermentation, as well as how these conditions affect bacterial population. The above should be included in future design in related work.

Conclusions

The two test strains are useful as starter cultures in the controlled fermentation of cabbage and soybeans to form useful products. Both *Pediococcus pentosaceus* and *B. subtilis* have capabilities to produce useful enzymes. Sequence alignment of 16S ribosomal RNA of the test strain confirmed the LAB as *Pediococcus pentosaceus* strain DSM20336 and *B. subtilis* subsp. *subtilis* strain 168. Results showed that *P. pentosaceus* induced ferments contained the lowest number of unwanted isolates in cabbage and soybean unlike in spontaneous fermentation where 8-9 unwanted isolates were found. The study identified potential fermenting strains of bacteria that produced quality ferments, reduced spoilage and prevented unwanted bacteria. These strains could be employed as starter culture in the industrial fermentation of vegetable and legume foods to boost food security in Nigeria.

References

Adedokun EO, Rather IA, Bajpai VK, Park YH. 2016. Biocontrol efficacy of *Lactobacillus fermentum* YML014 against food spoilage moulds using the tomato puree model. Frontiers in Life Science. 9: 64–68.

Ahmad A, Ramasamy K, Bakar A, Majeed A, Ahmad A, Ramasamy K, Bakar A, Majeed A, Mani V. 2015. Enhancement of secretase inhibition and antioxidant activities of tempeh, a fermented soybean cake through enrichment of bioactive aglycones. Pharmaceutical Biology. 53: 758–766.

Akanni GB, Naude Y, de Kock HL, Buys EM. 2018. Diversity and functionality of bacillus species associated with alkaline fermentation of Bambara groundnut (*Vigna subterranean* L. Verdc) into dawadawa-type African condiment. European Food Research and Technology. 244: 1147–1158.

Arteaga VG, Leffler S, Muranyi I, Eisner P, Schweiggert-Weisz U. 2021. Sensory profile, functional properties and molecular weight distribution of fermented pea protein isolate. CRFS Current Research in Food Science. 4: 1–10.

Cheesbrough M. 2006. Medical laboratory manual for tropical countries. Vol. 1. 2nd ed. UK: Cambridge press. pp. 292–300.

Du R, Ge J, Zhao D, Sun J, Ping W, Song G. 2018. Bacterial diversity and community structure during fermentation of Chinese sauerkraut with *Lactobacillus casei* 11MZ-5-1 by Illumina Miseq sequencing. Letter of Applied Microbiology. 66: 55–62.

Emkani M, Oliete B, Saurel R. 2022. Effect of lactic acid fermentation on legume protein properties, a review. Fermentation. 8(244): 1-41.

Florindo RN, Souza VP, Mutti HS, Camilo C, Regina L, Marana SR, Polikarpov I, Nascimento AS. 2018. Structural insights into glucosidase transglycosylation based on biochemical, structural and computational analysis of two gh1 enzymes from *Trichoderma harzianum.* New Biotechnology. 40: 218–227.

Garrido-Galand S, Asensio-Grau A, Calvo-Lerma J, Heredia A, Andrés A. 2021. The potential of fermentation on nutritional and technological improvement of cereal and legume flours: A review. International Food Research. 145: 110398.

Hui W, Hou Q, Cao C, Xu H, Zhen Y, Kwok L, Sun T, Zhang H. 2017. Identification of Microbial Profile of Koji Using Single Molecule, Real-Time Sequencing Technology. Journal of Food Science. 162: 143–1199.

Kiczorowski P, Kiczorowska B, Samolińska W, Szmigielski M, Mieczan AW. 2022. Effect of fermentation of chosen vegetables on the nutrient, mineral, and biocomponent profile in human and animal nutrition. Scientific Reports. 12: 13422.

Li KJ, Brouwer-Brolsma EM, Burton-Pimentel KJ, Vergères G, Feskens EJM. 2021. A systematic review to identify biomarkers of intake for fermented food products. Genes and Nutrition. 16(5): 1-17.

Li Y, Liu T, Zhao M, Zhong H, Luo W, Feng F. 2019. In vitro and in vivo investigations of probiotic properties of lactic acid bacteria isolated from Chinese traditional sourdough. Applied Microbiology and Biotechnology. 103: 1893–1903.

Liu X, Kokare C. 2017. Microbial enzymes of use in industry. In: Biotechnology of Microbial Enzymes. Elsevier: Amsterdam, The Netherlands. pp. 267–298.

Pino A, De Angelis M, Todaro A, Van Hoorde K, Randazzo CL, Caggia C. 2018. Fermentation of *Nocellara etnea* table olives by functional starter cultures at low salt concentrations. Frontiers of Microbiology. 9: 1125-1133.
Swain MR, Anandharaj M, Ray RC, Rani RP. 2014. Fermented Fruits and Vegetables of Asia: A Potential Source of Probiotics. Biotechnology Research International. 20(14): 1-19.
Taddia A, Boggione MJ, Tubio G. 2019. Screening of different agroindustrial by-products for industrial enzymes production by fermentation processes. International Journal of Food Science and Technology. 54: 1027–1035.
Vossen J, Tang S, Katase M. 2019. The use of next generation sequencing for improving food safety: Translation into practice. Food Microbiology. 79: 96–115.
Walters W, Hyde ER, Berg-Lyons D, Ackermann G, Humphrey G, Parada A, Gilbert JA, Jansson JK, Caporaso JG, Fuhrman JA. 2016. Improved Bacterial 16S rRNA Gene (V4 and V4-5) and Fungal Internal Transcribed Spacer Marker Gene Primers for Microbial Community Surveys. mSystems. 1: e00009-15.

BIOACTIVITY AND PHYTOCHEMISTRY OF *GUIERA SENEGALENSIS* J.F. GMEL. (COMBRETACAE)

Amna H.A. Atia[1*], Salar Hafez-Ghoran[2], P.D. Douanla[3], Sobia Ghani[2], S. Yousuf[2]

[1]Department of Microbiology and Parasitology, Medicinal and Aromatic Plants and Traditional Medicine Research Institute (MAPTMRI), National Center for Research, Khartoum-Sudan
[2]H.E.J. Research Institute of Chemistry, International Center for Chemical and Biological Sciences, University of Karachi, Karachi, Pakistan
[3]Department of Organic Chemistry, Faculty of Science, The University of Yaoundé-1, P.O. Box 812, Yaoundé, Cameroon
[*] Corresponding author e-mail: hamadamna6@gmail.com; AmnaAtia@ncr.gov.sd

Abstract

The phytochemical constituents of *Guiera senegalensis*, a widely used traditional medicinal plant in Africa, were investigated for their potential biological activities. Ethanolic extracts of *G. senegalensis* leaves were fractionated, and the resulting fractions were analyzed using GC-MS and NMR techniques. Forty compounds were identified by comparing their spectral data with published references. The hexane extract exhibited promising anti-leishmanial activity against *Leishmania major*, with an IC_{50} of 16.69 ± 0.3 µg/mL. The ethyl acetate fraction showed moderate activity (IC_{50} = 89.63 ± 0.6 µg/mL), while dichloromethane fractions were inactive at concentrations exceeding 100 µg/mL. The extract demonstrated limited antibacterial activity, inhibiting only *Bacillus subtilis* with a 60.31% inhibition rate, and showed no antifungal effects. Cytotoxicity testing on 3T3 cells revealed less than 50% inhibition, indicating minimal toxicity at tested concentrations. These findings support the ethnopharmacological relevance of *G. senegalensis* and highlight its potential as a source of anti-leishmanial drug candidates.
Keywords: *Guiera senegalensis,* spectral analysis, Bio-assay, Anti-leishmanial activity

Introduction

Natural products remain a vital source of chemical diversity for drug discovery, with medicinal plants offering a rich repository of bioactive compounds, including crude extracts, essential oils, and secondary metabolites (1). In Africa, many traditionally used medicinal plants remain understudied despite their therapeutic potential.

Guiera senegalensis, a shrub belonging to the Combretaceae family, is widely used in traditional African medicine, particularly across the Sahel region. It is employed in treating wounds, snakebites, gastrointestinal disorders, coughs, and neurological conditions such as Alzheimer's disease (2). These traditional uses have prompted increasing scientific interest in its phytochemistry and pharmacological properties. Previous studies have reported antioxidant, neuroprotective, and antibacterial effects from the ethanolic leaf extract, attributed to compounds such as flavonoids, alkaloids, and galloylquinic acid derivatives (3). GC-MS analysis has identified over 50 compounds in *G. senegalensis*, including significant

Received 3 April 2025; Reviewed 10 June 2025; Accepted 9 September 2025;
Published Online 9 September 2025; Published 30 September 2025

concentrations of flavonoids and alkaloids (4). These phytochemicals are known to exert antibacterial and antifungal activities, primarily through mechanisms like membrane disruption and enzyme inhibition (5).
Given the increasing threat of antimicrobial resistance and the global burden of leishmaniasis, there is an urgent need to identify novel therapeutic agents. This study investigates the phytochemical profile of *G. senegalensis* leaves and evaluates the biological activities of its extracts and fractions, with a focus on anti-leishmanial, antibacterial, and antifungal properties.
We hypothesize that the ethanolic leaf extract contains bioactive phytochemicals such as flavonoids, alkaloids, and terpenoids that exhibit antimicrobial and antiparasitic effects through mechanisms including membrane disruption, microbial enzyme inhibition, and interference with parasite metabolism. This study aims to isolate and identify these compounds and assess their biological activities to elucidate their potential modes of action.
The novelty of this study lies in its integrative approach, combining GC-MS and NMR-based phytochemical profiling with targeted bioactivity screening. Unlike prior studies, our work systematically links specific chemical fractions of *G. senegalensis* to anti-leishmanial and antimicrobial effects, providing new insights into its pharmacological potential.

Materials and Methods

Plant Collection and Authentication:
Guiera senegalensis leaves were collected from Darfur, Western Sudan, and authenticated by a taxonomist at the Herbarium of Medicinal and Aromatic Plants and Traditional Medicine Research Institute (MAPTRI), National Centre for Research (NCR), Khartoum, Sudan. A voucher specimen was deposited (Voucher No. KHT-SD-2022/43).
Extraction Procedure
The plant material was washed, air-dried, ground into powder, and stored at room temperature. One kilogram of powdered leaves was extracted with 80% ethanol using the maceration method described by Harborne (6). The extract was filtered, evaporated under reduced pressure, and the yield was calculated. Residues were stored at 4 °C in tightly sealed glass vials for further analysis.
Fractionation, Compound Isolation, and Purification
The crude ethanolic extract was partitioned sequentially using solvents of increasing polarity: n-hexane, dichloromethane (DCM), and ethyl acetate (EtOAc), using a separating funnel. Each fraction was concentrated, weighed (n-hexane: 14.29 g; DCM: 32.46 g; EtOAc: 38.14 g), and stored for chromatographic separation.
Column chromatography was performed using silica gel and a gradient solvent system (n-hexane–EtOAc–MeOH). Fractions (F1–F24) were collected and further purified by semi-preparative HPLC (RP-C18 column), using MeOH:H_2O (80:20) at a flow rate of 4 mL/min for 20 minutes. Isolated compounds were collected in pre-weighed, labeled vials and analyzed by thin-layer chromatography (TLC) (7).
The bio-active compounds were identified by GC-MS, and Nuclear magnetic resonance (NMR) spectral data. GC- MS were conducted using:
Gas chromatography- mass spectrum (GC-MS) analysis: Mass-Hunter GC/MS (Agilent Technologies, Santa Clara, CA, USA), equipped with a ZEBRON –ZB-5 column (430C: 30 m × 320 µm × 0.25 µm) and operated in electron ionization (EI) mode at 70 eV with a scan MS1 range of 40–700 m/z. Helium was used as the carrier gas (1.5 mL/min). The temperature of the inlet was set to 250 ◦C. The column temperature initiated at 50 ◦C for 5 min, and then was programmed to rise to 200 ◦C at the rate of 7 ◦C/min for 20 mi, then to raise 300 ◦C at the rate 7 ◦C/ min, for 30 min

Nuclear magnetic resonance (NMR) spectral data: One – dimensional (l^{1}H NMR), **two – dimensional(**2D), **and ^{13}C NMR,** spectra were recorded in CDCl3 or MeOD on AVANCE III 500 MHz spectrometer (Bruker, Switzerland) at 500 MHz using tetramethylsilane as an internal standard. The chemical shifts were given in δ (ppm). Their spectral data were then compared with published values and further conformed using NIST/EPA/NIH Mass spectral database (NIST11) to NIST MS search program v.2.0 g. (8).

Biological Assays:

Cell Line and Cytotoxicity screening

The cytotoxicity of the extracts and fractions was evaluated using 3T3 mouse fibroblast cells via the MTT colorimetric assay (9). Cells were seeded in 96-well plates and incubated with varying concentrations of test samples. After 24 hours, MTT (3-[4, 5-dimethylthiazol-2-yl]-2, 5-diphenyltetrazolium bromide) solution was added to each well and incubated for 4 hours. The resulting formazan crystals were dissolved in DMSO, and absorbance was measured at 540 nm using a micro-plate reader (Spectra Max Plus, Molecular Devices, CA, USA).

Cytotoxicity was expressed as the concentration causing 50% growth inhibition (IC_{50}). Percent inhibition was calculated using the formula:

Inhibition (%) = $100 - \left(\frac{\text{mean of O.D of test compound} - \text{mean of O.D of negative control}}{\text{mean of O.D of positive control} - \text{mean of O.D of negative control}}\right) \times 100$

OD test: Mean optical density of cells treated with test compound

OD negative: Mean OD of negative control (e.g., untreated cells = 100% viability)

OD positive. Mean OD of positive control (e.g., a known cytotoxic agent like doxorubicin = 0% viability). Data were processed using Soft Max Pro Software (Molecular Devices, USA).

Anti-Leishmanial Activity:

The anti-leishmanial activity of *G. senegalensis* extracts, fractions, and isolated compounds was evaluated against *Leishmania major* promastigotes (ATCC 50155) using a micro-plate-based assay (10). Promastigotes were incubated with test samples in RPMI-1640 medium supplemented with 10% fetal calf serum (FCS). Parasite viability was assessed by counting motile cells using a Neubauer chamber. IC_{50} values were calculated using EZ-Fit software based on dose-response curves (11)

Screening of plant extract on Amastigotes:

To evaluate intracellular activity, macrophage monolayers were prepared in 24-well plates (1×10^{6} cells/well) and infected with *L. major* promastigotes at a ratio of 5:1 (parasite: macrophage). After 48 hours of incubation, non-internalized parasites were removed, and infected macrophages were treated with test extracts. The following parameters were calculated:

Infection Rate (IR) = Number of infected macrophages in 100 macrophages

Multiplication Index (MI): = $\frac{\text{Number of amastigotes in test culture / 100 macrophages}}{\text{Number of amastigotes in control / 100 macrophages}}$ x 100

Antibacterial Activity:

Preparation of Bacterial Inoculum:

Antibacterial activity was tested against five bacterial strains (*E. coli*, *S. aureus*, *B. subtilis*, *P. aeruginosa*, and *S. typhi*) using the Microplate Alamar Blue Assay (MABA), as described by Sarker. (12). Bacterial suspensions were adjusted to 0.5 McFarland standard (~10^{8} CFU/mL), and diluted 1:10 in nutrient broth.

Microdilution Assay: 100 µL of nutrient broth was dispensed into each well of a sterile 96-well plate. Serial two-fold dilutions of extracts were prepared, followed by 100 µL of bacterial suspension and 10 µL of resazurin dye (0.01% w/v). Ciprofloxacin was used as the positive control. Plates were incubated at 37 °C for 18–24 h. Color change was visually inspected and quantitatively measured at 570 nm and 600 nm.

MIC Determination: The **Minimum Inhibitory Concentration (MIC)** was defined as the lowest concentration of the extract or fraction at which no visible color change (i.e., retention of blue color) occurred, indicating effective inhibition of bacterial growth.

Percentage Inhibition (%) = $\left(\frac{\text{A control} - \text{A blank}}{\text{A control} - \text{A test}}\right) \times 100$

***In-vitro* Anti-fungal activity Bioassay (Preliminary Screening)**:

The antifungal activity of *G. senegalensis* leaf extracts and fractions were evaluated against six fungal strains, *Aspergillus fumigatus* (ATCC 46645), *Aspergillus niger* (clinical isolate), *Candida albicans* (SC5314), *Candida glabrata* (ATCC 2001), *Fusarium lini* (environmental isolate), *Microsporum canis* (ATCC 36299), and *Trichophyton rubrum* (clinical isolate) using the broth microdilution method. (13), with minor modifications.

Preparation of Fungal Inoculum:

Fungal strains were cultured on Sabouraud Dextrose Agar (SDA) and incubated at 28 °C for 48-72 hours. Spores or yeast cells were harvested using sterile saline solution containing 0.05% Tween 80 and adjusted to a final concentration of approximately1 $\times 10^6$ spores/ml, using a hemocytometer.

Microdilution Assay:

In sterile 96-well micro-titer plates, 100 µL of Sabouraud Dextrose Broth (SDB) was dispensed into each well. Serial two-fold dilutions of the test extracts and fractions were prepared in the wells to achieve different concentrations. Subsequently, 100 µL of fungal inoculum was added to each well, with final volume 200 µL /well. The plates were incubated at 28°C for 48 hours under sterile conditions.

Assessment of Fungal Growth:

After incubation, fungal growth was assessed visually and by measuring linear growth (in mm). Additionally, 20µL of 0.01% (w/v) Resazurin solution was added to each well as a viability indicator. Blue-to-pink color shift indicated fungal viability and metabolic activity.

Determination of Antifungal Activity:

Antifungal efficacy was determined by calculating the percentage inhibition of fungal growth compared to the negative control. The % inhibition was calculated using the following formula:

% inhibition = $100 - \frac{\text{Linear growth in test (mm)}}{\text{Linear growth in Control (mm)}}$ x 100

The Minimum Inhibitory Concentration (MIC) Determination:

The MIC was defined as the lowest concentration of the test extract or fraction that resulted in no visible fungal growth or no color change in the resazurin dye, indicating complete growth inhibition.

Statistical Analysis:

All experiments were conducted in triplicate, and the results are presented as mean ± **standard deviation (SD). The inhibitory concentration (IC_{50})** values for both anti-leishmanial and cytotoxicity assays were calculated using dose response curves generated in Microsoft Excel. Absorbance readings at 540 mm were used to assess cell viability following treatment with varying concentration of plant extracts and fractions. Percentage inhibition (% inhibition) was calculated relative to untreated controls, and non-linear regression was applied to IC_{50} values. The IC_{50} was defined as the concentration of the test sample that resulted in 50% inhibition of parasite or cell viability. A p-value **<0.05 was considered statistically significant. For antibacterial and antifungal assays,** for antibacterial and antifungal assays, the percentage inhibition of microbial growth was calculated relative to untreated controls. Differences between treated and control groups were considered statistically significant at **p < 0.05.**

Results

Isolation and Identification of Bio-active compounds:

The bioactive compounds in *G. senegalensis* were identified through Gas Chromatography-Mass Spectrometry (GC-MS) analysis and Nuclear Magnetic Resonance (NMR) spectral data (1H, 2D, 13C NMR), along with mass spectral data and comparison with previously published data from the National Library of Medicine. The fractions of the ethanolic extract of *G. senegalensis* were analyzed using (^{1}H and ^{13}C NMR), mass spectral analysis, and GC-MS chromatography. Known compounds (40) were identified (Table 1, and Figures (1-40) supplementary file), by comparing their spectral data with previously reported data in the literature. As pure Compounds: **7 (**43 mg), Flavasperone (14) (Figure 1), **10**(34.5mg) as Ethyl gallate (3) (Figure 2), **32**(22 mg) as 1-Eicosanol, **(37)** as β –Amyrin, **38** (31 mg), as α-Amyrin (15) (Figures 3, 4, 5), and **40** (4.65mg) as Daucosterol (16) (Figure 6), while the other compounds were obtained as mixtures (Figure 7).

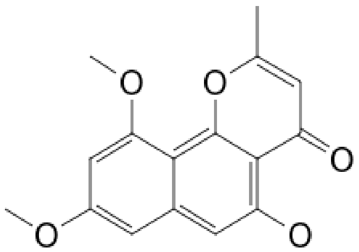

Figure 1. Structure of pure compound Flavasperone in *G senegalensis* J.F.Gmel.

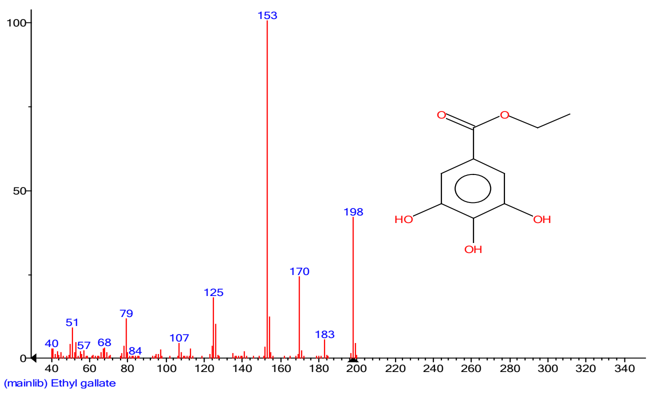

Figure 2. Mass spectrum of pure compound Ethyl gallate of hexane fraction

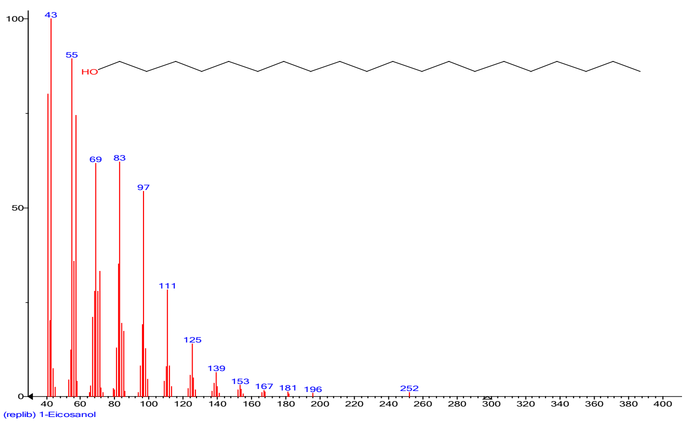

Figure 3. Mass spectrum of pure compound 1-Eicosanol of hexane fraction

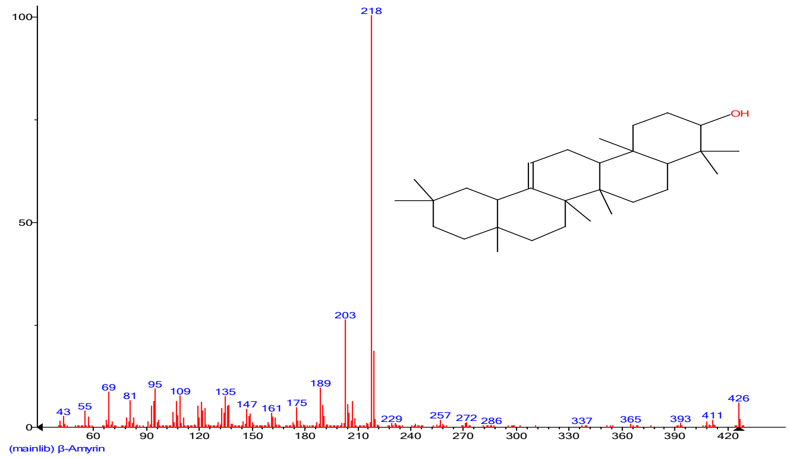

Figure 4. Mass spectrum of pure compound β-Amyrin of hexane fraction

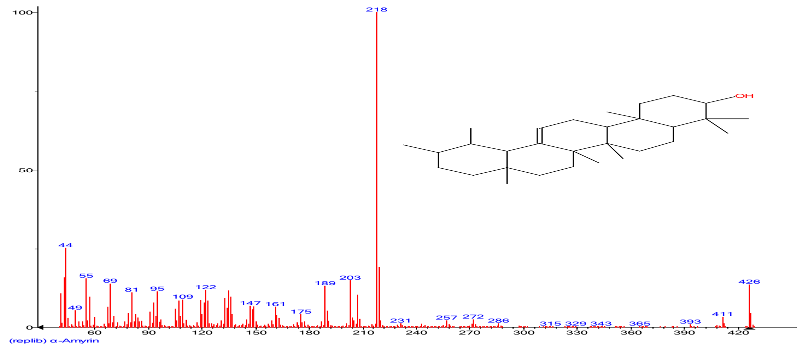

Figure 5. Mass spectrum of pure compound α-Amyrin of hexane fraction

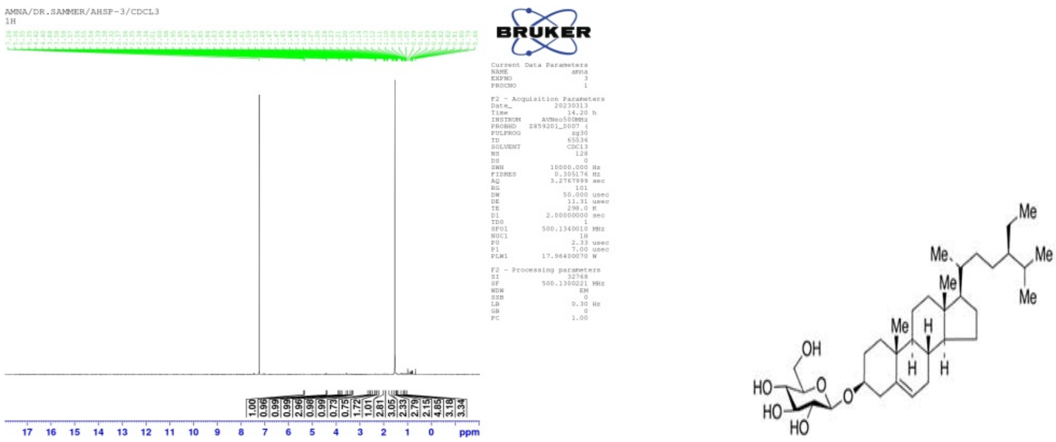

Figure 6. NMR spectra of compound Daucosterol of Ethyl acetate fraction

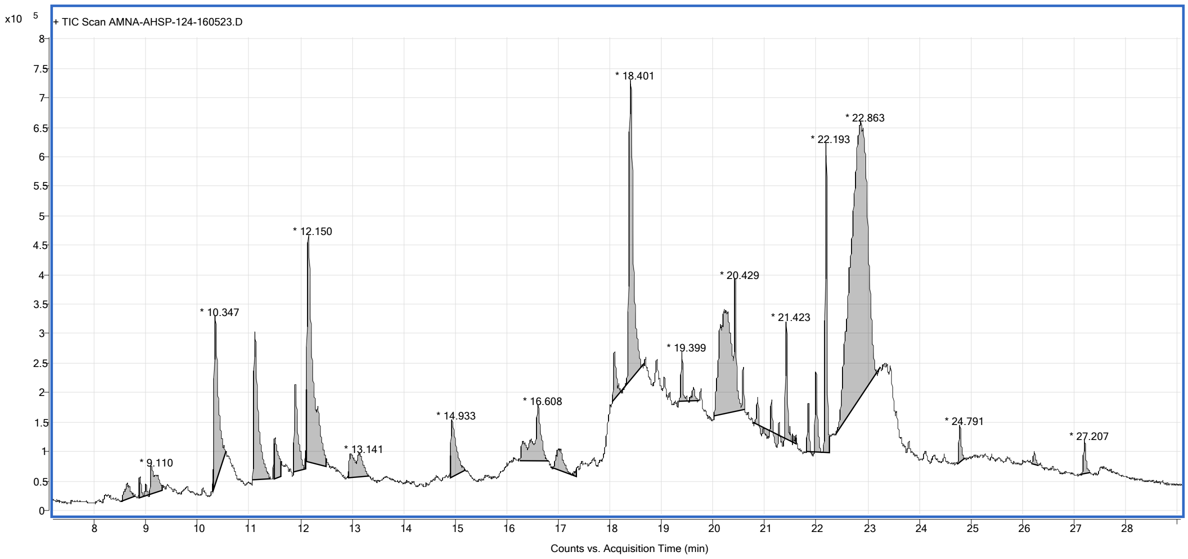

Figure 7. Mass spectrum of compounds mixture in *Guiera senegalensis* J.F.Gmel (Combretacae) leaves using GC-MS analysis

Cytotoxicity screening:
The cytotoxicity of the *G. senegalensis* extract was assessed alongside standard drugs (Table 1), and demonstrated less than 50% cytotoxicity against 3T3 cells, indicating no significant toxicity at the tested concentrations.

Table 1. Cytotoxicity of *G. senegalnesis* extract on 3T3 (Mouse fibroblast) cell evaluated by assay (MTT BI)

Test compound\s	**Concentration (µg\ml)**	**% inhibition**	**IC_{50} µg\ml± SD**
G. senegalensis crude extract	30 µg\ml	5.0%	In active (non- cytotoxic)
Doxorubicin(Control)	30 µg\ml	89.9%	0.2

Key: IC_{50} < 50 µg\ml: High toxic, > 50 µg/ml: no toxic *Control = standard drug/s (Doxorubicin) was used as the control positive at 0.1±0.02 µg/mL.

***In vitro* assessment of anti-leishmania activity**
The hexane fraction exhibited the highest anti-leishmanial activity against *L. major* promastigotes, with an IC_{50} of 16.69 ± 0.3 µg/mL. The ethyl acetate fraction had moderate activity (IC_{50} = 89.63 ± 0.6 µg/mL), while the DCM fraction and crude extract were inactive (IC_{50} > 100 µg/mL). Standard drugs amphotericin B and pentamidine had IC_{50} values of 3.39 ± 0.03 and 4.39 ± 0.01 µg/mL, respectively.

Table 2. *In vitro* anti-*leishmania* activity (*leishmania major) Promastigotes* of extract/ fractions of *G. senegalensis* and standard drugs

Test compound\s		**IC_{50} µg\ml± SD**	
crude extract		>100	In active
fractions	hexane	16.69±0.3	Significant active

	DCM	>100	In active
	Ethyl acetate	89.63 ±0.6	Low activity
Compound			
Standard Drug\s	Amphotericin B	3.39±0.03	Highly potent (Ref.)
	Pentamidine	4.39±0.01	Highly potent (Ref.)

Antibacterial activity:
The ethanolic extract of *G. senegalensis* showed **moderate antibacterial activity** against *Bacillus subtilis* (60.31% inhibition), but was **inactive** against the other strains. In contrast, standard antibiotics exhibited **broad-spectrum potency** with over 89% inhibition. The selective activity against *B. subtilis* suggests a potential affinity for Gram-positive bacteria, likely due to phytochemicals such as flavonoids or alkaloids. While less potent than conventional drugs, the extract's activity supports further **fractionation and optimization** to identify and enhance its active constituents (Table 2).

Table 3. Percentage inhibition of *G. senegalensis* of test bacterial strain vs. standard antibiotics

Bacterial Strain	% inhibition of test extract/compound	% inhibition of standard drug
Escherichia coli ATCC25922	-	89.20
Bacillus subtilis ATCC23857	60.31%	90.47
Staphylococcus aureus NCTC6571	-	90.37
Pseudomonas aeruginosa ATCC10145	-	92.42
Salmonella typhi ATCC 14028	-	96.62

***Key:** amount of extract 60 mg, Amount of drug: 10 mg, Con. of extract: 3000 µg/ml, Con. of drug: 1000 µg/ml.

Anti-fungal activity:
Based on the growth of various Fungus strains including *Aspergillus fumigatus*, *Aspergillus niger*, *Candida albicans*, *Candida glabarata*, *Fusarium lini*, *Microsporumcanis*, and *Trichophyton rubrum*, their linear growth (in mm) and growth inhibition were summarized in Table 2.

Discussions

Phytochemical analysis of *G. senegalensis* revealed rich profile of secondary metabolites, including flavonoids, tri-terpenes (α- and β-amyrin), sterols (daucosterol), and phenolic compounds such as ethyl gallate. These are widely recognized for their antimicrobial and anti-parasitic activities, which likely underpin the bioactivity observed in this study. Flavonoids are known to disrupt microbial membranes, interfere with nucleic acid synthesis, and alter energy metabolism, thereby exhibiting broad-spectrum antimicrobial properties (17). In the context of leishmaniasis, several flavonoids induce oxidative stress and mitochondrial dysfunction in *Leishmania* spp., leading to apoptotic-like cell death (18). Likewise, tri-

terpenes such as α- and β-amyrin have been shown to impair parasite membrane integrity and modulate host immune responses (19).
Among the tested extract and fractions, the hexane fraction exhibited the most potent anti-leishmanial activity (IC_{50} = 16.69 ± 0.3 µg/mL), supporting the presence of active non-polar constituents particularly tri-terpenoids and sterols. Although less potent than standard drugs Amphotericin B (IC_{50} = 3.39 ± 0.03 µg/mL) and Pentamidine (IC_{50} = 4.39 ± 0.01 µg/mL), the hexane fraction demonstrated significantly lower cytotoxicity, suggesting a more favorable therapeutic index. Key compounds (α-amyrin, β-amyrin, ethyl gallate, and daucosterol) were successfully isolated and are likely responsible for this activity. Their identification provides a promising foundation for further structural and mechanistic studies.
The extract also displayed selective antibacterial activity, against *Bacillus subtilis* (60.31% inhibition), consistent with the preferential action of flavonoids and alkaloids on gram-positive bacteria (16). While less effective than standard antibiotics (90-96% inhibition).this result supports further bio-guided purification. However, the extract did not exhibit significant antifungal activity, in contrast to earlier studies. The observed antifungal effect was modest and varied by strain, with partial inhibition noted against *Trichophyton rubrum* and *Fusarium lini*, while *Candida albicans* remained resistant. This aligns with previous findings suggesting that antifungal properties in *G. senegalensis* are associated with compounds such as guieranone A and phenolic acids (5). Against *Candida albicans*, remain inconsistent (20). While the extract has demonstrated antibacterial activity against *Staphylococcus aureus* and *Bacillus subtilis* (21).
Importantly, the isolation of specific compounds from the hexane fraction confirms the presence of pharmacologically relevant molecules with selective anti-parasitic activity. These findings position *G. senegalensis* as a promising candidate for the discovery of novel anti-leishmanial agents. Future efforts should focus on detailed mechanistic studies and in vivo validation to assess efficacy, safety, and potential for therapeutic development.
This study has limitations. All bioactivity assays were conducted *in vitro*, and the antimicrobial screening was limited to a select panel of pathogens. Therefore, further research including *in vivo* models and expanded microbial testing is essential to fully establish the clinical relevance and translational potential of *G. senegalensis* derived compounds.

Conclusions

This study highlights *G. senegalensis* as a promising source of bioactive compounds with selective anti-leishmanial properties. The hexane fraction, in particular, demonstrated significant activity against *Leishmania major* with low cytotoxicity, and the successful isolation of compounds such as α-amyrin, β-amyrin, ethyl gallate, and daucosterol strengthens its potential as a lead for drug development. Although the crude extract exhibited modest antimicrobial activity, its selective effect against Gram-positive bacteria supports further purification and optimization.

Acknowledgement: The authors express sincere gratitude to Hussin Ebrahim Jamal (HEJ) and the Research Institute of Chemistry at the University of Karachi in Pakistan for their invaluable support in providing the necessary facilities for conducting the analysis and anti-leishmanial studies. Special acknowledgement is owed to all the co-authors who provided assistance in bringing this study to completion.

References

1. Newman DJ, Cragg GM. 2020. Natural products as sources of new drugs over the nearly four decades from 01/1981 to 09/2019. J Nat Prod. 83(3): 770–803. https://doi.org/10.1021/acs.jnatprod.9b01285.
2. Dirar AI, Devkota HP. 2021. Ethnopharmacological uses phytochemistry and pharmacological activities of *Guiera senegalensis* J.F. Gmel. (Combretaceae). J Ethnopharmacol. 267: 113433. https://doi.org/10.1016/j.jep.2020.113433.
3. Bhat P, Patil VS, Anand A, Bijjaragi S, Hegde GR, Hegde HV, Roy S. 2023. Ethyl gallate isolated from phenol-enriched fraction of *Caesalpinia mimosoides* Lam. promotes cutaneous wound healing: A scientific validation through bioassay-guided fractionation. Front Pharmacol. 14: 1214220. https://doi.org/10.3389/fphar.2023.1214220.
4. Zayyan SM, Uba A, Faruq UZ, Izuagie T. 2024. Characterization and Phospholipase A_2 Inhibitory Potential of *Guiera senegalensis* Leaves Extracts via Experimental and Computational Approaches. Preprints (Preprint).
5. Moreira R, Ferreres F, Gil-Izquierdo Á, Gomes NGM, Araújo L, Pinto E et al. 2023. Antifungal activity of *Guiera senegalensis*: From the chemical composition to the mitochondrial toxic effects and tyrosinase inhibition. Antibiotics. 12(5): 869. https://doi.org/10.3390/antibiotics12050869.
6. Harborne JB. 1998. Phytochemical Methods: A Guide to Modern Techniques of Plant Analysis. 3rd ed. London: Chapman & Hall. Pp. 60–6.
7. Marston A, Hostettmann K. 1991. Thin-layer chromatography and bioautography of plant extracts and pure compounds. In: Dey PM, Harborne JB, editors. Methods in Plant Biochemistry: Plant Phenolics. Vol. 1. London: Academic Press. pp. 101–46.
8. Silverstein RM, Webster FX, Kiemle DJ, Bryce DL. 2014. Spectrometric Identification of Organic Compounds. 8th ed. Hoboken (NJ): John Wiley & Sons.
9. Mosmann T. 1983. Rapid colorimetric assay for cellular growth and survival: Application to proliferation and cytotoxicity assays. J Immunol Methods. 65(1–2): 55–63. https://doi.org/10.1016/0022-1759(83)90303-4.
10. Croft SL, Coombs GH. 2003. Leishmaniasis– current chemotherapy and recent advances in the search for novel drugs. Trends Parasitol. 19(11): 502–8. https://doi.org/10.1016/j.pt.2003.09.008.
11. Atta-ur-Rahman R, Chaudhary MI, Thompson W. 2001. Bioassay Techniques for Drug Development. Vol. 60. Amsterdam: Harwood Academic Publishers.
12. Sarker SD, Nahar L, Kumarasamy Y. 2007. Microtitre plate-based antibacterial assay incorporating resazurin as an indicator of cell growth, and its application in the in vitro antibacterial screening of phytochemicals. Methods. 42(4): 321–4. https://doi.org/10.1016/j.ymeth.2007.01.006.
13. Kumar S, Yadav A, Yadav M, Yadav JP. 2016. Antimicrobial properties of various parts of *Guazuma ulmifolia* Lam. against clinical pathogens. BMC Complement Altern Med. 16: 173. https://doi.org/10.1186/s12906-016-1141-4.
14. Abdelwahab GM, Mira A, Cheng YB, Abdelaziz TA, Lahloub MFI, Khalil AT. 2021. Acetylcholine esterase inhibitory activity of green synthesized nanosilver by naphthopyrones isolated from marine-derived *Aspergillus niger*. PLoS One. 16(9): e0257071. https://doi.org/10.1371/journal.pone.0257071.
15. Gil Archila E, Rojas-Bautista F, Garcia N, Carvajal Vasquez JA. 2022. A promising blueberry from Colombia: Antioxidant activity, nutritional and phytochemical composition of *Cavendishia nitida* (Kunth) A.C.Sm. Heliyon. 8(5): e09448. https://doi.org/10.1016/j.heliyon.2022.e09448.

16. Rajavel T, Mohankumar R, Archunan G, Ruckmani K, Devi KP. 2017. Beta sitosterol and daucosterol (phytosterols identified in *Grewia tiliaefolia*) perturb cell cycle and induce apoptotic cell death in A549 cells. Sci Rep. 7(1): 3418. https://doi.org/10.1038/s41598-017-03511-4.
17. Cushnie TPT, Lamb AJ. 2011. Recent advances in understanding the antibacterial properties of flavonoids. Int J Antimicrob Agents. 38(2): 99–107.
18. Sen R, Bandyopadhyay S. 2011. Activities of flavonoids as potential anti-leishmanial agents: A review. Pharm Biol. 49(5): 442–9.
19. Nery CGC, de Morais SM, da Costa WAK, Pereira PR, Silva ARA, da Silva M et al. 2017. Antileishmanial activity of ursolic acid and oleanolic acid derivatives. Bioorg Med Chem Lett. 27(7): 1791–4.
20. Jiyil MK, Mafuyai CE, Shago MI, Inuwa HM. 2019. Antimicrobial activity of methanolic, aqueous and partially purified protein of young and matured leaves of *Guiera senegalensis* (Moshi medicine). J Adv Med Pharm Sci. 1–11.
21. Saidu T, Galadima M, Jigam A, Abalaka E. 2016 Antibacterial and potential toxicological evaluation of leaf extracts of *Guiera senegalensis* against Gram-negative bacteria. J Adv Med Pharm Sci. 9(1): 1–13. https://doi.org/10.9734/JAMPS/2016/25815.

TOXICOLOGICAL ASSESSMENT OF CARBON NANOMATERIALS ON *LEMNA MINOR* L.: INSIGHTS INTO PHYSIOLOGICAL AND BIOCHEMICAL ALTERATIONS

Ștefan Mihăiță Olaru[1*], Maria-Magdalena Zamfirache[1]

[1]Faculty of Biology, "Alexandru Ioan Cuza" University of Iasi, Romania
[*] Corresponding author e-mail: stefan.olaru@uaic.ro

Abstract

Synthetic carbon-based nanomaterials, such as multi-walled carbon nanotubes (MWCNTs), carboxyl-functionalized nanotubes (MWCNTs-COOH), and fullerene soot, are increasingly being utilised in practical industrial and agricultural applications. This reality raises concerns about their potential unfavourable ecotoxicological impact on aquatic ecosystems where they may accidentally end up. In this context, the present research aimed to evaluate several physiological and biochemical responses of plants belonging to the species *Lemna minor* L. when interacting with these types of nanomaterials, experimentally added at two concentrations (50 and 200 mg/L) to their culture medium over a 14-day cultivation period.
The results obtained demonstrated the appearance in the test plants of functional effects dependent on the dose and nature of the tested nanomaterial, reflected by significant changes in photosynthetic performance (decreases in the content of photo-assimilatory pigments and the efficiency of photosystem II), as well as by the activation of biochemical markers of oxidative stress (increases in the content of flavonoids and polyphenols, changes in POD and SOD activities). The functionalized nanotubes (MWCNTs-COOH) induced the most pronounced biochemical responses, while fullerene soot had more moderate effects, possibly due to its reduced bioavailability in the cultivation media.
The results highlight the sensitivity of *Lemna minor* to chemical stress generated by synthetic carbon-based nanomaterials present in the cultivation medium, thus confirming its usefulness as a model organism in ecotoxicological studies and emphasising the need for rigorous assessments regarding the potential impact of these nanomaterials on aquatic plants in natural ecosystems, to lay the groundwork for responsible ecological management strategies.
Keywords: *Lemna minor*, carbon nanomaterials, oxidative stress, photosynthesis, aquatic ecotoxicology

Introduction

Nanotechnologies represent an emerging field of modern science with remarkable application potential in agriculture, biomedicine, industry, and environmental protection. Their relevance derives from the possibility of designing materials with specific physicochemical properties at the nanoscale (Fang et al. 2017, Patel et al. 2020, Mathew and Victório 2022). Carbon nanotubes (CNTs) stand out due to their unique tubular structure, small dimensions, superior electrical conductivity, and chemical stability, being widely used in laboratory experiments and innovative applications. In the agricultural sector, CNTs have been tested to promote plant growth by improving water and nutrient absorption, as well as serving as vectors for delivering genes and bioactive substances to plant organs (Tan et al. 2009, Jordan et al. 2020). However,

Received 22 July 2025; Reviewed 4 September 2025; Accepted 6 September 2025;
Published Online 9 September 2025; Published 30 September 2025

the widespread use of these nanomaterials has raised concerns regarding their potential toxicity to biological systems, including plants. The effects of CNTs on plant organisms are often contradictory, ranging from stimulating physiological processes to inducing oxidative stress due to the production of reactive oxygen species (Mittler 2002, Chen et al. 2018, Ren et al. 2021, Samadi et al. 2021). In the context of increasingly intense anthropogenic pollution of terrestrial and aquatic ecosystems, synthetic carbon-based nanomaterials are emerging as a potentially omnipresent category of environmental contaminants. This trend is driven by their rapidly expanding industrial applications (Jackson et al. 2013).

In efforts to assess the impact of these nanomaterials on plants, morphological and physiological studies constitute an essential step in elucidating the response mechanisms of vegetation exposed to these compounds. Although numerous studies have investigated CNT interactions with microorganisms, protozoa, or algae, their effects on higher aquatic plants remain poorly understood. In this context, plants from the Lemnoideae subfamily, particularly specimens of the species *Lemna minor* L., are recognized as model organisms in ecotoxicity tests due to their favourable biological characteristics for practical research activities: rapid vegetative reproduction, pollutant bioaccumulation capacity, high ecological tolerance to pollutants, and an important role in phytoremediation (Nasu and Kugimoto 1981, Bokhari et al. 2016, Lanthemann and van Moorsel 2022).

Although species such as *Lemna minor* are well established in studies on wastewater remediation and in monitoring of classic contaminants (e.g., heavy metals, pesticides, dyes), specialised literature still highlights a lack of data on their interaction with CNT-type nanomaterials. Moreover, in the case of microplastic pollution, published results generally indicate a low morpho-physiological impact on *Lemna* colonies, despite their significant bioaccumulation potential. These findings underscore the need to expand knowledge on the effects of CNMs on aquatic plants, particularly concerning the structure and function of their photosynthetic apparatus, redox homeostasis, and overall metabolic dynamics. Given this context, the present study investigates physiological and biochemical responses of *Lemna minor* exposed to synthetic carbon-based nanomaterials, in experimental conditions simulating possible contamination scenarios of natural aquatic environments. By addressing these aspects, the results aim to clarify the bioindicator potential of *Lemna minor* in relation to emerging pollutants and contribute to a better understanding of the ecotoxicological risks associated with the uncontrolled release of nanomaterials into freshwater ecosystems.

Materials and Methods

Nanomaterials

Multi-walled carbon nanotubes (MWCNTs) with an outer diameter of 8 nm (purity > 96%, product code NG01MW0101) and carboxylated MWCNTs (MWCNTs-COOH) with an outer diameter of 8–18 nm (purity > 96%, product code NG01MW0303) were purchased from Nanografi (Ankara, Turkey), while fullerene soot, consisting of a mixture of C_{60}, C_{70} fullerenes, and carbon black (product code 572497-5G), was obtained from Sigma-Aldrich.

Cultivation of *Lemna minor* L. plants

For the experiments, the cultivation protocol for *Lemna minor* L. species followed the recommendations of OECD guideline No. 221 regarding growth tests with *Lemna* spp. (OECD 2006). The base culture was maintained under controlled laboratory conditions (24 ± 2°C, artificial lighting for 17 h/day, light intensity 115–118 μmol m^{-2} s^{-1}), being periodically transferred to fresh media to avoid nutrient depletion and accumulation of residual metabolites. To obtain experimental cultures with reduced phenotypic variability, secondary stock cultures were created starting from a single individual (monoclonal cultures). From these, the plants used in the exposure tests were selected, each cultivation well with culture medium (10 ml volume) receiving a single individual with three fronds. The wells were placed in trays covered with black paint to limit algae development and were incubated at 25°C, with the same lighting regime as previously described, for a cultivation period of 14 days. To ensure the reproducibility and biological relevance of the test, which requires a uniform dispersion of nanoparticles without their aggregation, the CNMs were ultrasonicated. The culture medium in the experimental variants was supplemented with concentrations of 50 and 200 mg/L of each type of CNM tested, and the control variants contained only the simple culture medium. The concentrations were selected based on values commonly applied in ecotoxicological studies with nanomaterials, ensuring both comparability with existing literature and experimental reproducibility. This range was intended to simulate possible contamination scenarios in aquatic ecosystems while providing insights into potential dose-dependent physiological and biochemical effects in *Lemna minor*. Plant development was monitored every 2–3 days throughout the cultivation period, with physiological and biochemical determinations performed at the end (14 days).

Determination of stomatal density

Stomatal density was evaluated by scanning electron microscopy (SEM) on intact leaves/fronds collected at the end of the experiment, selected from morphologically and ontogenetically equivalent regions of all experimental variants. Samples were fixed in 2.5% glutaraldehyde in 0.1 M phosphate buffer (pH 7.2) for 2 hours at room temperature, then rinsed and dehydrated in a graded series of acetone (30–100%). After critical point drying with liquid CO_2, fragments were mounted on metal supports with conductive adhesive tape and coated with gold (~10 nm) by sputtering (Pathan et al. 2010). Observations were made with a Tescan Vega II SBH SEM microscope at 30 kV, analysing at least three biological replicates per variant and at least three fields per replicate. Stomatal density (stomata/mm²) was calculated based on SEM micrographs with known magnification (Xu and Zhou 2008).

Determination of chlorophyll fluorescence

The functioning of the photosynthetic apparatus of the test plants was evaluated by determining the quantum efficiency of photosystem II (ΦPSII), using a Hansatech FMS II portable fluorimeter. Measurements were made by bringing the device's optical fibre to about 1 cm from the surface of the leaves/fronds, with five readings taken for each experimental variant.

Obtaining plant extracts for biochemical analyses, the leaves/fronds were homogenised in a mortar with quartz sand and 10 ml of solvent (96% ethanol for quantifying photo-assimilatory pigments and secondary metabolites; TRIS-HCl for determining enzymatic activity - SOD and POD and for quantifying protein content), according to the methods described by Wellburn and Artenie (Wellburn 1994, Artenie et al. 2008). The resulting plant extracts were centrifuged for 15 minutes at 4000 rpm at a temperature of 4°C. Determinations were performed in technical triplicate for each of the three cultivated biological replicates, and the results were expressed as arithmetic means.

Determination of photo-assimilatory pigment content

The content of chlorophyll a, chlorophyll b, and carotenoid pigments was determined spectrophotometrically, with readings at wavelengths of 664, 648, and 470 nm of the plant extracts (Wellburn 1994, Zhao et al. 2017). The calculation of pigment concentrations was performed using standard formulas:

$$\text{Chl a} = 13{,}36 \times A_{664} - 5{,}19 \times A_{648}$$

$$\text{Chl b} = 27{,}43 \times A_{648} - 8{,}12 \times A_{664}$$

$$\text{Cx+c} = (1000 \times A_{470} - 2{,}13 \times \text{Chl a} - 97{,}64 \times \text{Chl b}) / 209$$

Total polyphenol content was quantified using the Folin-Ciocalteu method (Herald et al. 2012). Plant extracts were treated with Folin-Ciocalteu reagent and 7.5% sodium carbonate, and their absorbance was read spectrophotometrically at λ= 765 nm. The content was expressed in mg gallic acid equivalents (GAE)/g fresh material, using a standard curve.

Total flavonoid content was determined by the aluminium chloride method (Herald et al. 2012), by measuring the absorbance of treated plant extracts at λ = 510 nm. Results were expressed in mg quercetin equivalents (QE)/g fresh material.

Antioxidant activity was evaluated using the DPPH test (Sharma and Bhat 2009, Behrendorff et al. 2013). Plant extracts were incubated with 60 µM DPPH solution, and their absorbance was read after 3 hours of incubation at λ = 517 nm. Antioxidant capacity was expressed as percentage inhibition of DPPH radicals, compared to an ascorbic acid control.

Superoxide dismutase (SOD) activity was determined according to the Nitro Blue Tetrazolium (NBT) method, by inhibiting NBT photoreduction by superoxide radicals generated with riboflavin (Artenie et al. 2008). Absorbance of plant extracts was measured spectrophotometrically at λ = 560 nm, and SOD activity was expressed in active enzyme units/gram fresh material.

Peroxidase (POD) activity was determined according to the Winterbourn method adapted by Artenie et al. (Winterbourn et al. 1975, Artenie et al. 2008), by measuring the oxidation of ortho-dianisidine under the action of peroxidase and H_2O_2. Absorbance of plant extracts was determined spectrophotometrically at λ = 540 nm and expressed in POD units/minute/gram fresh material.

Protein content was assayed using the Bradford method (Artenie et al. 2008), with spectrophotometric readings at λ = 595 nm. Results were reported against a standard curve built with bovine serum albumin (BSA).

Statistical analysis of the experimental data was performed using one-way ANOVA with Tukey's post hoc test ($p < 0.05$).

Results and discussions

Stomatal density

Exposure of *Lemna minor* plants to multi-walled carbon nanotubes (MWCNTs) resulted in a moderate increase in their stomatal density, dependent on the tested dose, alongside a significant reduction of individual stomatal surface area (Figure 1). This phenomenon suggests an adaptive mechanism of stomatal miniaturisation in test plants under the abiotic stress conditions. Similar but more pronounced effects were observed with MWCNTs-COOH treatment, indicating an amplified phytotoxic potential of carboxyl groups (Verneuil et al. 2015). Contrary to these trends, fullerene soot treatment reduced stomatal density but increased their surface area, reflecting an alternative compensatory mechanism to maintain optimal gaseous exchange in duckweed plants exposed to these synthetic carbon-based nanomaterials in the cultivation environment. These stomatal modifications highlight the capacity of *Lemna minor* to register structural changes under nanomaterial-induced stress, reinforcing its utility as a morphological bioindicator for detecting sublethal effects of emerging aquatic pollutants, in line with specialised literature reporting stress-induced stomatal patterns characterised by increased density and reduced dimensions. (Xu and Zhou 2008, de Morais et al. 2019).

Chlorophyll fluorescence (ΦPSII)

The efficiency of photosystem II progressively decreased in the test plant leaves/fronds during the experiment, with the most severe effect observed in the MWCNTs-COOH treatment at a concentration of 200 mg/l (Figure 2A). At lower doses, MWCNTs-COOH treatment induced reduced toxicity in *Lemna minor* plants, likely due to better dispersion and lower particle aggregation in the growth medium. Fullerene soot caused only moderate declines in ΦPSII, suggesting limited physical interaction with chloroplasts in the plant's vegetative structures. The decline in ΦPSII efficiency confirms the sensitivity of *Lemna minor* to photochemical disruption caused by carbon nanomaterials. Such measurable changes in photosynthetic performance can validate its role as a physiological bioindicator in ecotoxicological studies (Chen et al. 2018, Ozfidan-Konakci et al. 2022).

Photo-assimilatory pigments content

Treatments with MWCNTs and MWCNTs-COOH caused quantitative decreases in chlorophylls and carotenoid pigments in *Lemna minor* leaves/fronds, proportional to the applied dose (Figure 2B), indicating varied phytotoxic effects. Fullerene soot at 200 mg/l induced the most pronounced decline in photo-assimilatory pigments in test plants. This effect likely results from either reduced light penetration caused by surface particle aggregation or intensified oxidative stress impacting pigment-producing cells. Dose-dependent pigment reductions reveal *Lemna minor*'s sensitivity to light stress and oxidative damage, confirming its value as a bioindicator of environmental stress (Lang et al. 2019, Subotić et al. 2022).

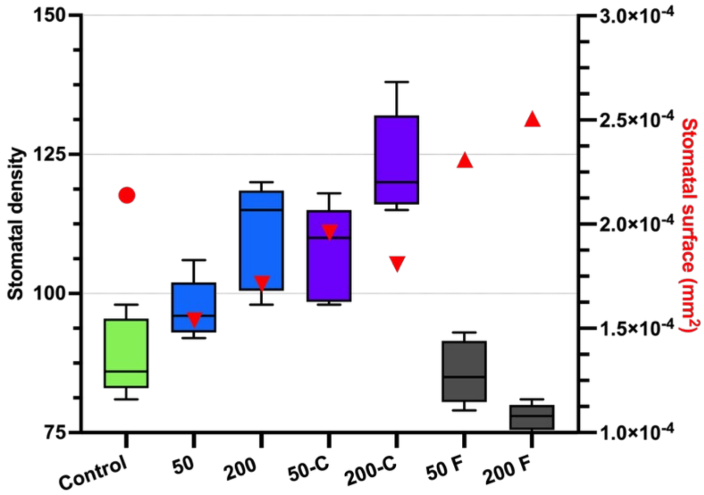

Figure 1. Stomatal density of *Lemna minor* L. individuals cultivated under experimental conditions. Variants: Control, 50 - 50 mg/l MWCNT, 200 – 200 mg/l MWCNT, 50-C – 50 mg/l MWCNT-COOH, 200-C - 200 mg/l MWCNT-COOH, 50 F – 50 mg/l Fullerene soot, 200 F – 200 mg/l Fullerene soot. Statistically significant differences are observed in the case of 50, 200, 50-C, 200-C, and 200F. The stomatal area is marked on the secondary axis (in red) (● - control, ▲ - significant increase in stomatal area, ▼ - significant decrease in stomatal area).

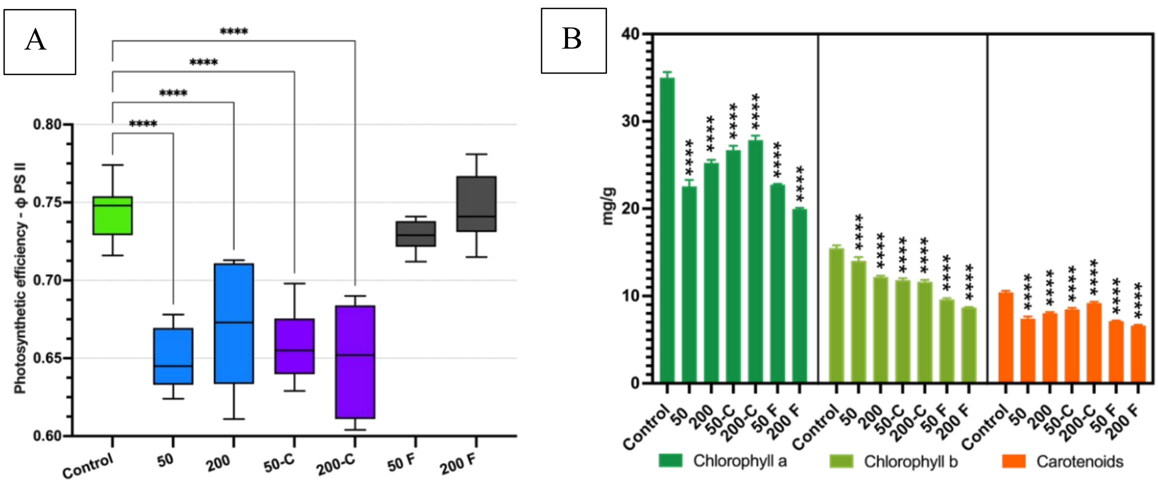

Figure 2. A-Efficiency of the photosynthetic apparatus, B-Assimilatory pigment content of *Lemna minor* L. individuals cultivated under experimental conditions. Variants: Control, 50 - 50 mg/l MWCNT, 200 – 200 mg/l MWCNT, 50-C – 50 mg/l MWCNT-COOH, 200-C - 200

mg/l MWCNT-COOH, 50 F – 50 mg/l Fullerene soot, 200 F – 200 mg/l Fullerene soot. Statistically significant differences are marked with *.

Flavonoid content

MWCNTs-COOH treatments significantly stimulated flavonoid biosynthesis in test plants, particularly at the concentration of 200 mg/l (Figure 3A), indicating an intense response to experimentally induced oxidative stress in the cultivation medium. Unfunctionalized MWCNTs and fullerenes caused a decrease in these compounds, demonstrating a weak effect; the obtained results are consistent with data presented in specialised literature (Chen et al. 2020).

Polyphenol content

All tested nanomaterials experimentally added to the cultivation medium of *Lemna minor* plants induced the biosynthesis of high polyphenol content (Figure 3B), with MWCNTs-COOH treatment at 200 mg/l concentration standing out among experimental variants. The high levels of polyphenol content suggest an important antioxidant role of this group of compounds in ROS detoxification in test plants. Fullerene soot had a weak effect, likely due to its low solubility. (Gohari et al. 2020). Enhanced flavonoid and polyphenol accumulation in *Lemna minor* under nanomaterial stress indicates antioxidant mechanisms activation, highlighting its sensitivity to redox imbalance and utility as a bioindicator of oxidative stress in aquatic systems.

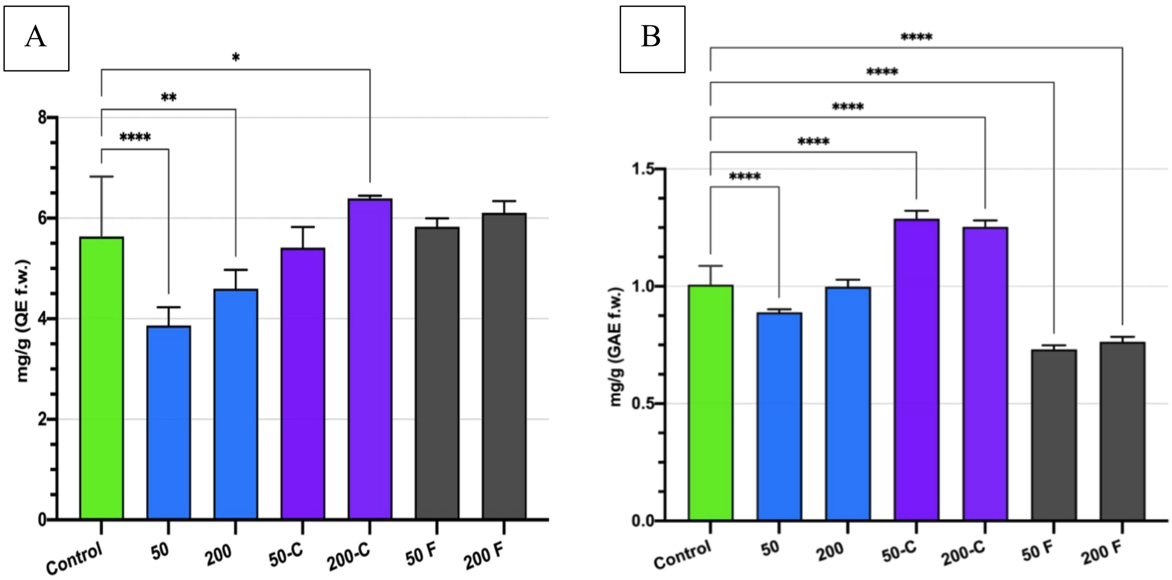

Figure 3. A-Flavonoid content, B-Polyphenol content of *Lemna minor* L. individuals cultivated under experimental conditions. Experimental variants: Control, 50 - 50 mg/l MWCNT, 200 – 200 mg/l MWCNT, 50-C – 50 mg/l MWCNT-COOH, 200-C - 200 mg/l MWCNT-COOH, 50 F – 50 mg/l Fullerene soot, 200 F – 200 mg/l Fullerene soot. Statistically significant differences are marked with *.

Peroxidase activity (POD)

Treatments with MWCNTs and MWCNTs-COOH reduced POD activity, especially in variants with 200 mg/l concentration (Figure 4A), indicating inhibition of the enzymatic antioxidant system in test plants. In the case of fullerene soot testing, POD values remained close to control levels, suggesting moderate stress manifestation in *Lemna minor* plants and conserved enzymatic function (Dietz and Herth 2011).

Superoxide dismutase activity (SOD)

All tested nanomaterials induced decreased SOD activity in test plants (Figure 4B), with the most severe effect observed in treatments with 200 mg/l concentrations. This SOD activity inhibition indicates a possible major redox imbalance in plant structures and an inability to efficiently detoxify the superoxide (Gill and Tuteja 2010).

Soluble protein content

Non-functionalized and functionalized carbon nanotubes caused a decrease in protein content of *Lemna minor* plants (Figure 5), more pronounced in treatment variants with a concentration of 200 mg/l. Fullerene soot induced a hormetic effect: a decrease in protein content at 50 mg/l and a partial recovery at 200 mg/l, suggesting compensatory adaptation mechanisms of test plants to experimentally induced abiotic stress in the cultivation medium (Calabrese and Agathokleous 2021). Reduced POD and SOD activities together with protein depletion reveal impaired antioxidant and metabolic functions in *Lemna minor*, reinforcing its value as a biochemical bioindicator of nanomaterial-induced stress.

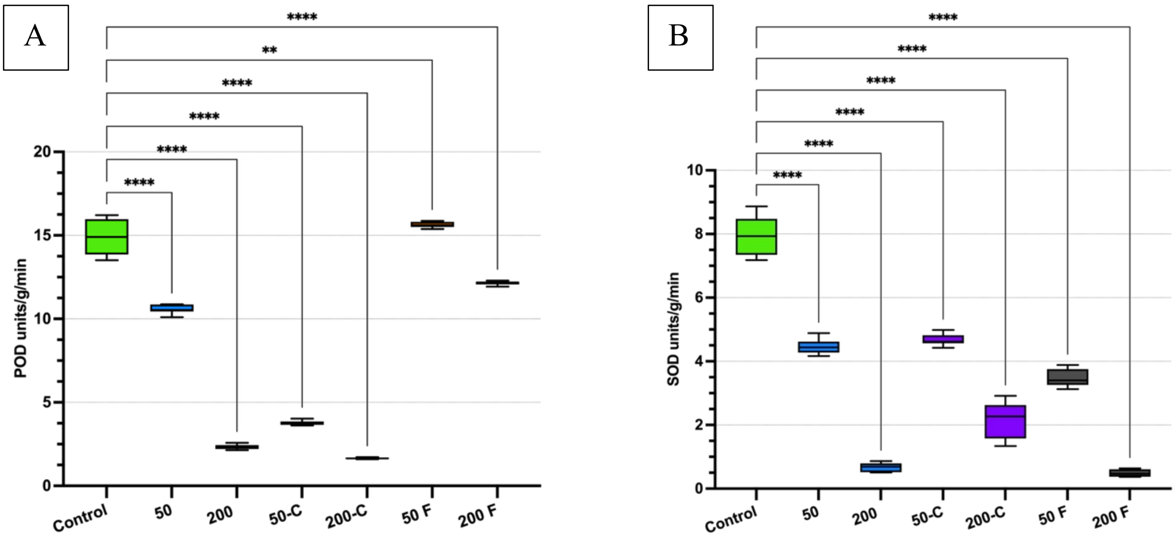

Figure 4. A-POD activity, B-SOD activity of *Lemna minor* L. individuals cultivated under experimental conditions. Experimental variants: Control, 50 - 50 mg/l MWCNT, 200 – 200 mg/l MWCNT, 50-C – 50 mg/l MWCNT-COOH, 200-C - 200 mg/l MWCNT-COOH, 50 F – 50 mg/l Fullerene soot, 200 F – 200 mg/l Fullerene soot. Statistically significant differences are marked with *.

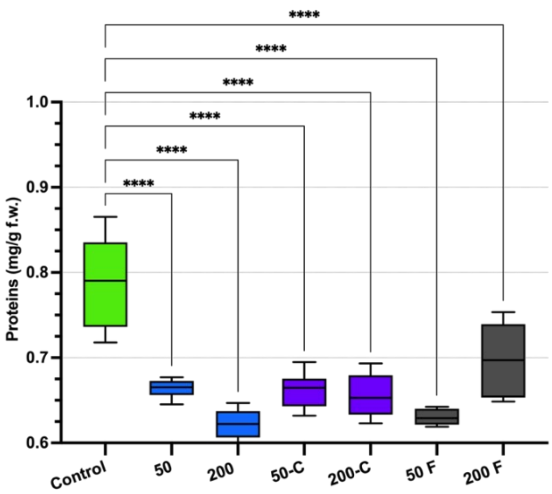

Figure 5. Soluble protein content of *Lemna minor* L. individuals cultivated under experimental conditions. Experimental variants: Control, 50 - 50 mg/l MWCNT, 200 – 200 mg/l MWCNT, 50-C – 50 mg/l MWCNT-COOH, 200-C - 200 mg/l MWCNT-COOH, 50 F – 50 mg/l Fullerene soot, 200 F – 200 mg/l Fullerene soot. Statistically significant differences are marked with *.

Total antioxidant activity

This biochemical parameter increased significantly in the MWCNTs and MWCNTs-COOH treatment variants at a concentration of 200 mg/l, confirming the induction of systemic oxidative stress in plant structures by these nanomaterials (Figure 6). The highest values of total antioxidant activity were observed when applying the MWCNTs-COOH treatment at a dose of 200 mg/l, while fullerene soot generated a nonlinear response, indicating the influence of nanoparticle aggregation on their bioavailability and absorption in test plants. The alteration of antioxidant activity under high-dose treatments demonstrates systemic stress response mechanisms. This parameter provides a robust biochemical signal, confirming *Lemna minor*'s effectiveness in early detection of nanomaterial-induced toxicity. (Zhang et al. 2017).

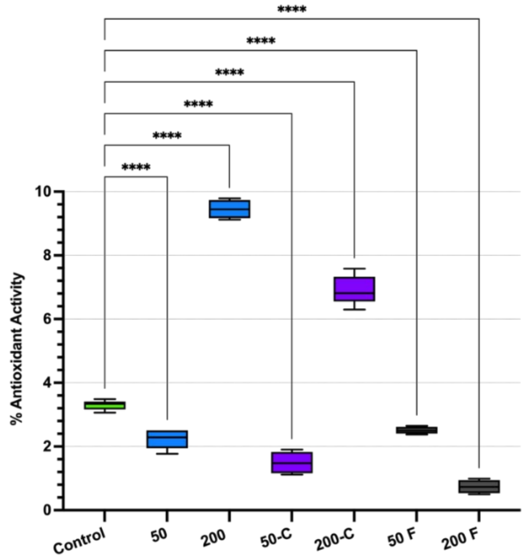

Figure 6. Total antioxidant activity of *Lemna minor* L. individuals cultivated under experimental conditions. Experimental variants: Control, 50 - 50 mg/l MWCNT, 200 – 200 mg/l MWCNT, 50-C – 50 mg/l MWCNT-COOH, 200-C - 200 mg/l MWCNT-COOH, 50 F – 50 mg/l Fullerene soot, 200 F – 200 mg/l Fullerene soot. Statistically significant differences are marked with *.

Conclusions

The results highlight a visible phytotoxicity, manifested across multiple physiological and biochemical levels, of the tested synthetic carbon-based nanomaterials – multi-walled carbon nanotubes (MWCNTs), carboxyl-functionalized nanotubes (MWCNTs-COOH), and fullerene soot – on the aquatic species *Lemna minor* L. The effects produced on the test plants are dependent on the chemical nature of the nanomaterials and the applied dose, confirming that these nanoparticles profoundly influence plant metabolism and the functional integrity of their photosynthetic apparatus.

Stomatal modifications, reduction of assimilatory pigment content, and decreased photosystem II efficiency (ΦPSII) demonstrate severe impairment of photosynthetic performance in duckweed plants exposed to high concentrations of MWCNTs and MWCNTs-COOH, indicating disruptions in electron transport and degradation of chloroplast structures caused by oxidative stress occurring in plant tissues. In the same context, the increased accumulation of phenols and flavonoids in test plants, as an effect of MWCNTs-COOH treatments, suggests a compensatory activation of their antioxidant defences, while fullerene soot generated weaker metabolic responses, possibly due to its limited interaction with plant tissues. These results outline a specific response pattern of test plants to the experimentally induced abiotic stress in the aquatic environment, where effect severity is dictated by dose and nanomaterial surface chemistry, with photochemical and biochemical indicators representing potential reliable markers of these nanoparticles' phytotoxicity in aquatic environments. In the context of increasingly frequent use of functionalized nanomaterials across various fields, the obtained results emphasise the importance of rigorous assessment of these nanoparticles' impact on aquatic ecosystems. The experimental evidence presented in this study consolidates the role of *Lemna minor* as a highly responsive bioindicator for aquatic nanotoxicology. Its ability to exhibit measurable and dose-dependent changes in stomatal patterning, pigment composition, photosynthetic efficiency, antioxidant activity, and enzymatic function underlines its diagnostic value in detecting sublethal stress induced by carbon-based nanomaterials. The present findings underscore the necessity of implementing stringent regulatory frameworks governing the practical use of nanomaterials in order to prevent their accidental or uncontrolled release into the environment.

Acknowledgments: We would like to thank the Faculty of Biology from “Alexandru Ioan Cuza” University of Iasi for providing access to the Tescan Vega II SBH Microscope and the CERNESIM L2 Laboratory for providing some of the material resources used for this study.

References

Artenie V, Ungureanu E, Negură AM. 2008. Metode de investigare a metabolismului glucidic și lipidic – manual de lucrări practice. Editura PIM, Iași.

Behrendorff J, Vickers C, Chrysanthopoulos PhD P, Nielsen L. 2013. 2,2-Diphenyl-1-picrylhydrazyl as a screening tool for recombinant monoterpene biosynthesis. Microb Cell Factories. 12: 76. doi:10.1186/1475-2859-12-76.

Bokhari SH, Ahmad I, Mahmood-Ul-Hassan M, Mohammad A. 2016. Phytoremediation potential of *Lemna minor* L. for heavy metals. Int J Phytoremediation. 18(1): 25–32. doi:10.1080/15226514.2015.1058331.

Calabrese EJ, Agathokleous E. 2021. Accumulator plants and hormesis. Environ Pollut. 274: 116526. doi:10.1016/j.envpol.2021.116526.

Chen M, Zhou S, Zhu Y, Sun Y, Zeng G, Yang C, Xu P, Yan M, Liu Z, Zhang W. 2018. Toxicity of carbon nanomaterials to plants, animals and microbes: Recent progress from 2015-present. Chemosphere. 206: 255–264. doi:10.1016/j.chemosphere.2018.05.020.

Chen Q, Chen L, Nie X, Man H, Guo Z, Wang X, Tu J, Jin G, Ci L. 2020. Impacts of surface chemistry of functional carbon nanodots on the plant growth. Ecotoxicol Environ Saf. 206: 111220. doi:10.1016/j.ecoenv.2020.111220.

Dietz K-J, Herth S. 2011. Plant nanotoxicology. Trends Plant Sci. 16(11): 582–589. doi:10.1016/j.tplants.2011.08.003.

Fang S, Shen L, Zhang X. 2017. Chapter 9 - Application of Carbon Nanotubes in Lithium-Ion Batteries. In: Peng H, Li Q, Chen T, editors. Industrial Applications of Carbon Nanotubes. Boston: Elsevier. (Micro and Nano Technologies). pp. 251–276. [accessed 2025 May 6]. https://www.sciencedirect.com/science/article/pii/B9780323414814000095.

Gill SS, Tuteja N. 2010. Reactive oxygen species and antioxidant machinery in abiotic stress tolerance in crop plants. Plant Physiol Biochem. 48(12): 909–930. doi:10.1016/j.plaphy.2010.08.016.

Gohari G, Safai F, Panahirad S, Akbari A, Rasouli F, Dadpour MR, Fotopoulos V. 2020. Modified multiwall carbon nanotubes display either phytotoxic or growth promoting and stress protecting activity in *Ocimum basilicum* L. in a concentration-dependent manner. Chemosphere. 249: 126171. doi:10.1016/j.chemosphere.2020.126171.

Herald TJ, Gadgil P, Tilley M. 2012. High-throughput micro plate assays for screening flavonoid content and DPPH-scavenging activity in sorghum bran and flour. J Sci Food Agric. 92(11): 2326–2331. doi:10.1002/jsfa.5633.
Jackson P, Jacobsen NR, Baun A, Birkedal R, Kühnel D, Jensen KA, Vogel U, Wallin H. 2013. Bioaccumulation and ecotoxicity of carbon nanotubes. Chem Cent J. 7(1): 154. doi:10.1186/1752-153X-7-154.
Jordan JT, Oates RP, Subbiah S, Payton PR, Singh KP, Shah SA, Green MJ, Klein DM, Cañas-Carrell JE. 2020. Carbon nanotubes affect early growth, flowering time and phytohormones in tomato. Chemosphere. 256: 127042. doi:10.1016/j.chemosphere.2020.127042.
Lang J, Melnykova M, Catania M, Inglot A, Zyss A, Mikruta K, Firgolska D, Wieremiejczuk A, Książek I, Serda M, et al. 2019. A water-soluble [60]fullerene-derivative stimulates chlorophyll accumulation and has no toxic effect on *Chlamydomonas reinhardtii*. Acta Biochim Pol. doi:10.18388/abp.2019_2835. [accessed 2025 May 3]. https://www.frontierspartnerships.org/articles/10.18388/abp.2019_2835/pdf.
Lanthemann L, van Moorsel SJ. 2022. Species interactions in three Lemnaceae species growing along a gradient of zinc pollution. Ecol Evol. 12(2): e8646. doi:10.1002/ece3.8646.
Mathew S, Victório CP. 2022. Carbon Nanotubes Applications in Agriculture. In: Abraham J, Thomas S, Kalarikkal N, editors. Handbook of Carbon Nanotubes. Cham: Springer International Publishing. p. 1579–1593. [accessed 2025 May 6]. https://doi.org/10.1007/978-3-030-91346-5_35.
Mittler R. 2002. Oxidative stress, antioxidants and stress tolerance. Trends Plant Sci. 7(9): 405–410. doi:10.1016/S1360-1385(02)02312-9.
de Morais MB, Barbosa-Neto AG, Willadino L, Ulisses C, Calsa Junior T. 2019. Salt Stress Induces Increase in Starch Accumulation in Duckweed (*Lemna aequinoctialis*, Lemnaceae): Biochemical and Physiological Aspects. J Plant Growth Regul. 38(2): 683–700. doi:10.1007/s00344-018-9882-z.
Nasu Y, Kugimoto M. 1981. Lemna (duckweed) as an indicator of water pollution. I. The sensitivity of *Lemna paucicostata* to heavy metals. Arch Environ Contam Toxicol. 10(2): 159–169. doi:10.1007/BF01055618.
Oecd. 2006. Test No. 221: *Lemna* sp. Growth Inhib Test Guidel Test Chem.:1–26.
Ozfidan-Konakci C, Alp FN, Arikan B, Balci M, Parmaksizoglu Z, Yildiztugay E, Cavusoglu H. 2022. The effects of fullerene on photosynthetic apparatus, chloroplast-encoded gene expression, and nitrogen assimilation in *Zea mays* under cobalt stress. Physiol Plant. 174(3): e13720. doi:10.1111/ppl.13720.
Patel DK, Kim H-B, Dutta SD, Ganguly K, Lim K-T. 2020. Carbon Nanotubes-Based Nanomaterials and Their Agricultural and Biotechnological Applications. Materials. 13(7): 1679. doi:10.3390/ma13071679.
Pathan AK, Bond J, Gaskin RE. 2010. Sample preparation for SEM of plant surfaces. Mater Today. 12: 32–43. doi:10.1016/S1369-7021(10)70143-7.
Ren L, Wang M-R, Wang Q-C. 2021. ROS-induced oxidative stress in plant cryopreservation: occurrence and alleviation. Planta. 254(6): 124. doi:10.1007/s00425-021-03784-0.
Samadi S, Asgari Lajayer B, Moghiseh E, Rodríguez-Couto S. 2021. Effect of carbon nanomaterials on cell toxicity, biomass production, nutritional and active compound accumulation in plants. Environ Technol Innov. 21: 101323. doi:10.1016/j.eti.2020.101323.
Sharma OP, Bhat TK. 2009. DPPH antioxidant assay revisited. Food Chem. 113(4): 1202–1205. doi:10.1016/j.foodchem.2008.08.008.
Subotić A, Jevremović S, Milošević S, Trifunović-Momčilov M, Đurić M, Koruga Đ. 2022. Physiological Response, Oxidative Stress Assessment and Aquaporin Genes Expression of Cherry Tomato (*Solanum lycopersicum* L.) Exposed to Hyper-Harmonized Fullerene Water Complex. Plants. 11(21): 2810. doi:10.3390/plants11212810.

Tan X, Lin C, Fugetsu B. 2009. Studies on toxicity of multi-walled carbon nanotubes on suspension rice cells. Carbon. 47(15): 3479–3487. doi:10.1016/j.carbon.2009.08.018.
Verneuil L, Silvestre J, Mouchet F, Flahaut E, Boutonnet J-C, Bourdiol F, Bortolamiol T, Baqué D, Gauthier L, Pinelli E. 2015. Multi-walled carbon nanotubes, natural organic matter, and the benthic diatom *Nitzschia palea*: "A sticky story." Nanotoxicology. 9(2): 219–229. doi:10.3109/17435390.2014.918202.
Wellburn AR. 1994. The Spectral Determination of Chlorophylls a and b, as well as Total Carotenoids, Using Various Solvents with Spectrophotometers of Different Resolution. J Plant Physiol. 144(3): 307–313. doi:10.1016/S0176-1617(11)81192-2.
Winterbourn CC, Hawkins RE, Brian M, Carrell RW. 1975. The estimation of red cell superoxide dismutase activity. J Lab Clin Med. 85(2): 337–341.
Xu Z, Zhou G. 2008. Responses of leaf stomatal density to water status and its relationship with photosynthesis in a grass. J Exp Bot. 59(12): 3317–3325. doi:10.1093/jxb/ern185.
Zhang H, Yue M, Zheng X, Xie C, Zhou H, Li L. 2017. Physiological Effects of Single- and Multi-Walled Carbon Nanotubes on Rice Seedlings. IEEE Trans Nanobioscience. 16(7): 563–570. doi:10.1109/TNB.2017.2715359.
Zhao Q, Ma C, White JC, Dhankher OP, Zhang X, Zhang S, Xing B. 2017. Quantitative evaluation of multi-wall carbon nanotube uptake by terrestrial plants. Carbon. 114: 661–670. doi:10.1016/j.carbon.2016.12.036.